UNIVERSITY OF TURKU

Renewable energy system at shipyard

Master of Science in Technology Thesis

University of Turku
Department of Mechanical and Materials Engineering
Materials Engineering
Materials of Energy Technology

Author:
Rasmus Pulkkanen

Supervisors:
Associate professor Pekka Peljo D.Sc. (Tech.)
Juha Mikola M.Sc. (Tech.)

23.05.2024
Turku

Master of Science in Technology Thesis
University of Turku
Department of Mechanical and Materials engineering
Materials Engineering

Subject: Materials Engineering
Author: Rasmus Pulkkanen
Title: Renewable energy system at shipyard
Supervisors: Associate professor Pekka Peljo and Electricity Network Specialist Juha Mikola
Number of pages: 78 pages
Date: 23.05.2024

Abstract

The use and integration of renewable energy sources into business operations is becoming more common and their integration in the maritime industry will be essential in the future. Making this change voluntarily while being one of the leaders in the industry can further strengthen a company's reputation and competitive position, and also access to subsidies and funding can also be improved.

Through a comprehensive analysis of technological developments, and economic considerations, this thesis aims to provide useful insights into the implementation of renewable energy systems in shipyard environments. In this thesis, different solar and wind power systems were analysed under different scenarios, where electricity price, system price, system size and system location were variables.

In addition to economic considerations, the social aspect of sustainability must be taken into account when designing renewable energy systems. Ultimately, the decision to invest in renewables reflects a commitment to both environmental sustainability and long-term business success in an increasingly environmentally aware world.

The economic results did not reveal a situation where immediate investments are required, with the majority of results generating a payback time of more than 10 years. The results show that traditional horizontal wind power is more profitable than silicon solar panels or vertical wind power. However, the profitability of wind power is significantly affected by wind speed and only a slight change in wind speed could have a decisive impact on the final results. The values of levelized cost of energy for silicon solar panels were slightly below 10 cents/kWh regardless of the orientation or the angle of the panels, but with wind power values below 5 cents/kWh was reached.

Key words: renewable energy, photovoltaics, wind power, shipyard, feasibility.

Table of contents

Nomenclature

Abbreviation	Explanation
Wh	Watthour
PV	Photovoltaics
TFSC	thin film solar cells
α-Si	amorphous-silicon
CdTe	cadmium telluride
CIGS	copper indium gallium selenide
TCO	transparent conducting layer
PSC	perovskite solar cell
HTL	hole transporting layer
ETL	electron transporting layer
BIPV	building-integrated photovoltaics
HAWT	horizontal-axis wind turbine
VAWT	vertical-axis wind turbine
BIWT	building-integrated wind turbine
AWE	airborne wind energy
PCM	phase change materials
VAT	Value-added tax
PVGIS	Photovoltaic Geographical Information System
LCOE	levelized cost of energy
NPV	net present value

1 Introduction

In recent years, various industries have invested in sustainability and its integration into business operations. This is driven by the need to reduce the negative impacts of climate change and reduce dependence on limited fossil fuel resources. The maritime sector, which is known for its significant contribution to global emissions and pollution, will also face the challenge of integrating sustainability sooner or later in the form of regulations. Shipyards play a huge role in the maritime sector and their dependence on fossil fuels causes considerable environmental and economic damage. Therefore, the transformation of shipyard operations through the integration of renewable energy systems would contribute to the sustainability and resilience of the maritime sector. By doing this voluntarily whilst being a leader in the sector, the company's reputation and competitive position would be even stronger and access to subsidies could be easier.

This thesis is done for Meyer Turku as a commission and is part of the NEcOLEAP project. Meyer Turku is one of the biggest and most advanced shipbuilding companies in the world. About 15% of the world's cruise construction industry is accounted for by Meyer Turku. The NEcOLEAP research and development project aims to secure the competitiveness of the Finnish shipbuilding industry and a high level of cruise ship expertise and knowledge for the future. This will be achieved by bringing together members of industry, universities, and research institutes to develop sustainable and innovative technology solutions on a global scale. [1]

Renewable energies can be divided into solar energy, wind energy, hydro energy, marine energy, geothermal energy, and bioenergy. This thesis focuses on the first two and consists of two parts. Chapters 2,3 and 4 focus on the theoretical part, with a comprehensive review of the current and future potential of renewable energy sources and energy storage possibilities. Chapter 5 covers the case analysis of Meyer Turku and the implementation of a renewable energy system. The main goal of this thesis is to build a comprehensive literature review on these renewable energy systems and to answer the following research question: How is energy management structured within the shipyard, considering both consumption and production? What systems could be implemented to enhance energy production within the shipyard? What are the potential economic, and social benefits of transitioning towards renewable energy systems at shipyards?

2 Solar power

Solar energy is one of the largest, most efficient, and environmentally friendly renewable energy sources for electricity production. Solar energy is not only abundant but also the most common permanent energy source on our planet. Its applications go beyond its direct exploitation and include indirect methods such as wind, hydro, and biomass. [2] This chapter will focus primarily on its direct exploitation and the many ways in which it can be harnessed. In addition to its prevalence, solar energy is most evenly distributed around the world. As shown in Figure 1, solar irradiation varies across latitudes and climatic conditions, peaking at the Tropic of Cancer and Capricorn. In the context of this thesis, it's crucial to distinguish between irradiance and irradiation. Irradiance refers to the momentary power of the sun measured in watts per square meter (W/m^2) falling on a surface at any given moment. Whereas, irradiation represents the total amount of solar energy, measured in watt-hours per square meter (Wh/m^2), received by a surface over a specified period.

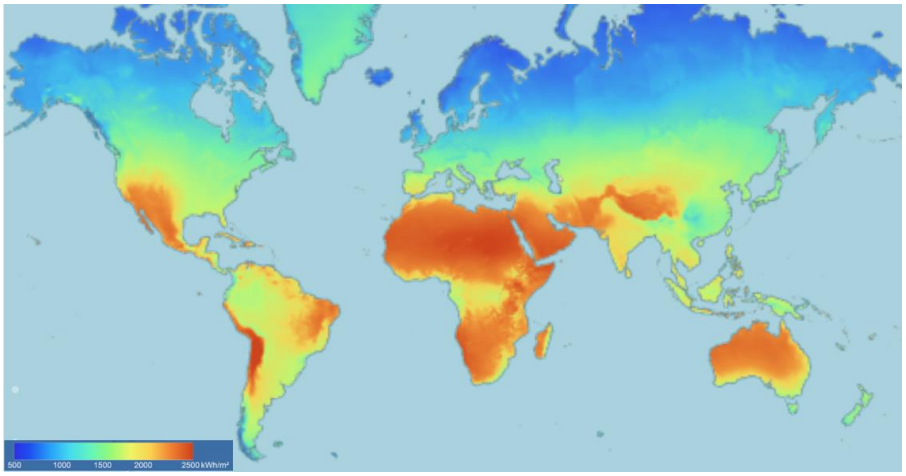

Figure 1. Solar irradiation across the world [3]. *© 2024 PVGIS.*

The global potential of solar power is enormous. The solar power in Earth's orbit can be calculated using the following equation.

$$P\ (solar\ power) = G_{SC}\ (solar\ constant) * \pi * r^2 (Earth\ radius)$$

The solar constant is the amount of total solar radiation per unit area, measured from a surface perpendicular to the Sun's rays at about the same distance as the Earth is from the Sun. The average solar constant between 2003 and 2020 was 1360.883 W/m^2 [4]. The Earth's equatorial radius is 6378.140 km, its polar radius is 6356.755 km and the global average is generally considered to be 6 371 km [5].

$$P = 1360.883\ \frac{W}{m^2} * \pi * (6\ 371\ 000\ m)^2$$

$$P = 173\ 534\ 517\ 181\ 502\ 099\ \text{W} = 174\ 000\ \text{TW}$$

There is approximately 174 000 TW of solar power in Earth's orbit, but only 51% of this reaches the Earth's ground level. The remaining 49% is either reflected by the atmosphere, clouds, and Earth's surface, or absorbed by the atmosphere and clouds. [6] Consequently, the actual solar power available at ground level is approximately 85 000 TW.

In 2022, global energy consumption reached approximately 177 000 TWh [7]. In terms of power, this equates to 20.20 TW. During the same year, solar energy production reached a new record of almost 1 300 TWh. In terms of power, this equates to 0.15 TW. Solar energy is therefore about 4 200 times greater than global energy consumption and about 566 000 times greater than current solar energy production. Essentially, solar power provides more energy to Earth in a few hours than the planet consumes in an entire year.

Figure 2 illustrates the amount of Earth's surface area that would need to be covered with solar panels and associated equipment to meet the energy needs of the entire planet. It's important to note that this estimation solely considers the total energy output by the panels and doesn't address the synchronization of production with consumption at any given moment or account for the spacing required between the panels. The approximate area needed is around 500 000 km^2.

Figure 2. The amount of Earth's surface area (yellow) that would need to be covered with solar panels and associated equipment to meet the energy needs of the entire planet. Reproduced under CC BY 4.0 license from ref. [9].

Concentrating solar-thermal power and photovoltaics (PV) are the two primary categories of solar energy technologies. Solar photovoltaics are used to directly convert sunlight into energy, while solar thermal collectors are used to heat water, air, or other fluids depending on the application. Concentrating solar-thermal power uses a variety of methods to capture solar thermal energy for use in thermal processes associated with electricity generation [10].

2.1 Concentrating solar power

Although the principle of concentrated solar power is relatively simple, it has been studied for several decades. At its core lies the utilization of mirrors, which serve to redirect, concentrate, and capture solar radiation, converting it into heat. This thermal energy can then be utilized to power generators or heat engines, thereby generating electricity. Solar collectors can be divided into two categories: stationary and sun-tracking. Stationary collectors are non-concentrated which means that incoming radiation is intercepted and absorbed in the same area. Sun-tracking collectors are concentrated, which means that they utilize optical elements to concentrate radiation in the receiving area. This involves tracking the sun throughout the day so that the solar radiation can be concentrated as accurately as possible at any given moment. [10]

The main types of stationary solar collectors are flat plate collectors and compound parabolic collectors while the main types of tracking collectors are parabolic trough collectors, parabolic dish collectors, heliostat field collectors, and linear Fresnel reflectors [11].

The flat-plate collector operates within a single level, resembling a box. It consists of a transparent lid, several pipes, and highly insulating materials. Inside the flat plate collector is a dark surface with a high absorption capacity. Solar energy is absorbed by this surface and transferred to the circulating liquid within the pipes. The liquid inlets and outlets are located at the corners of the collector, facilitating the flow. In contrast, a compound parabolic collector takes the form of a sharply bent reflecting plate, resembling a parabolic shape. This design enables light rays to be reflected multiple times within the collector, eventually reaching its bottom surface. Consequently, these collectors can capture solar radiation from various angles, enhancing their efficiency. [11]

The parabolic trough collector system consists of several sheets bent into a slightly parabolic shape and made of reflective material. The receiver is mounted in the linear focus of the long modules i.e., focus of parabola. Typically, the receiver consists of a black metal tube coated with a selective material and enclosed within a glass tube to minimize heat loss via convection.

To enhance transmittance, the glass tube is often coated with an anti-reflection coating. Thermal energy collected by the receiver is then transferred via a heat transfer fluid passing through it, supplying power generation systems. Additionally, parabolic trough collectors can be integrated with solar cells. These cells are typically mounted at the bottom of the parabolic shape, where they absorb solar flux, further enhancing energy capture efficiency. [10], [11]

In Nordic countries, where solar intensity is comparatively lower, stationary collectors and parabolic troughs are the only viable options as they are capable of efficiently producing heat within the temperature range of 50-300°C. Other types of collectors require a higher solar intensity to be profitable. Regular flat-plate collectors are most common but based on studies and calculations carried out in Potsdam, northeast Germany, 2021 [12] and Aalborg, northern Denmark, 2013 [13], the annual expected yield of parabolic collectors would be up to 500 kWh/m^2 at temperatures of 50-100 °C. This exceeds the output of a regular flat-plate collectors. However, it is worth noting that parabolic collectors need direct sunlight to work optimally. Since almost half of the sunlight in southern Finland is diffused, parabolic collectors may not achieve significant popularity in Finland [14].

2.2 Photovoltaics

2.2.1 Working principle

The photovoltaics involves the use of solar cells to generate electricity directly via the photovoltaic effect. Solar cells are based on semiconductors and as the name suggests, semiconductors are materials that do not naturally conduct electricity but are not insulators either. Figure 3 illustrates the difference in band gap between conductors, semiconductors, and insulators.

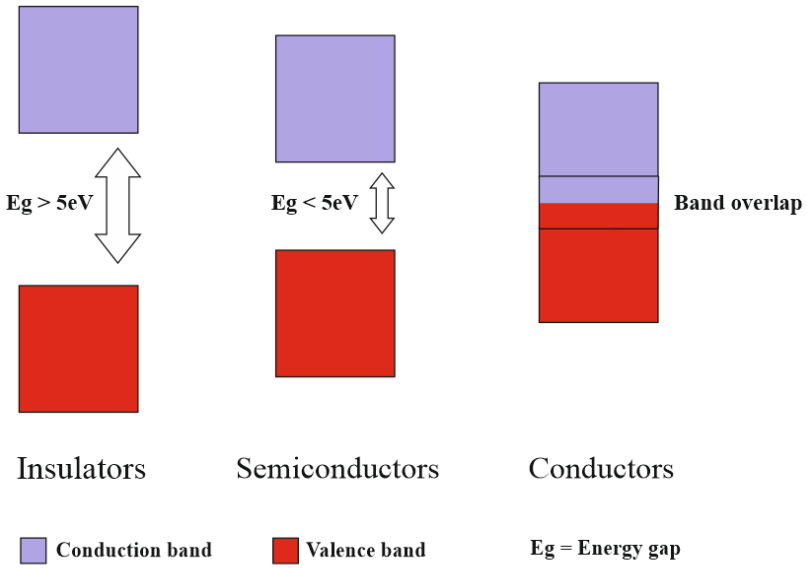

Figure 3. Differences in band gaps between insulators, semiconductors, and conductors.

In conductors, the lack of a band gap leads to an overlap of conductive and valence bands, which allow unrestricted electron movement. The amount of band overlap directly correlates with the material's conductivity. In contrast, insulators exhibit significant band differences, preventing electron excitation from the valence to the conduction band. Semiconductors, with a less bandgap, allow for electron excitation through solar radiation, or photons. When photons elevate an electron to the conduction band, the following electrons fill the vacancy, generating an electric current as photons create electron-hole pairs. The separated electron and hole move to the negative and positive poles, respectively. The band gap size affects the voltage, with larger gaps correlating to higher voltages while the current is related to the number of electrons excited by the photons. [15]

The charge separation occurs in the p-n junction, which is formed when p- and n-type semiconductors are in contact with each other, resulting in homojunction (same material layers) or heterojunction (different materials). P-n junctions in homojunction solar cells rely on doping, where impurity atoms are added to the lattice. Doping with boron or phosphorus alters the band gap, creating donor and acceptor states for efficient charge transfer. As a result of doping p-type semiconductors have higher density of holes in the valence band and n-type semiconductors have higher electron density in the conduction band. When a p-n junction is formed, the higher electron concentration of the n-type semiconductor compared to the p-type semiconductor causes the diffusion of negative carriers from the n-type semiconductor to the p-type semiconductor and vice versa, holes diffuse from the p-type to the n-type. Charge diffusion occurs until thermal equilibrium is achieved, creating a depletion area, and generating

an electric field. This electric field facilitates charge drift towards the n-side for electrons and the p-side for holes, establishing equilibrium when drift and diffusion currents are equal. [15], [16]

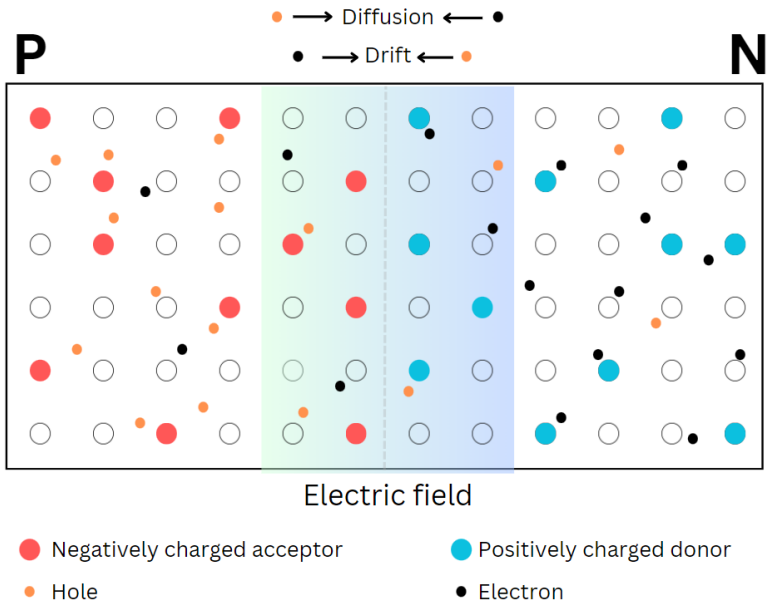

Figure 4. p-n junction and electric field. The blue circles are positively charged donors and the red circles are negatively charged acceptors. The black circles are electrons, and the orange circles are holes. The electric field is generated when equilibrium is achieved.

Examining the absorption and transfer mechanism, photons with energy equal to or greater than the semiconductor's band gap create electron-hole pairs in an excited state. Insufficient photon energy remains unexploited and may result in excess energy release through thermalization, heating the material lattice. Subsequently, the electron-hole pair diffuses or drifts towards the collection electrode. Collected charges recombine, vaporising energy as heat. Alternatively, recombination can emit photons, leading to new electron-hole pairs in direct bandgap materials with high purity. This process, responsible for charge transport, differs from diffusion or drift processes, offering insights into the complexities of semiconductor behaviour in harnessing solar energy for electricity generation. [17]

In heterojunction cells, a junction is formed between semiconductors with varying band gaps. One widely used heterojunction configuration combines hydrogenated amorphous silicon with crystalline silicon, often known as SHJ or silicon heterojunction. This heterojunction silicon cell forms its junction by depositing layers of crystalline silicon and hydrogenated amorphous silicon using plasma-enhanced chemical vapor deposition. The hydrogenated amorphous silicon layers are doped with opposite charges, transforming into charge-selective contacts.

These contacts play a crucial role in enabling the targeted transfer of specific charge carriers while effectively blocking the transfer of opposing charges. This surface passivation reduces recombination and significantly improves the open circuit voltage. Remarkably, silicon heterojunctions, especially when paired with homojunction passivated emitter rear locally-diffused solar cells, have demonstrated excellent performance among silicon-based photovoltaics. [17]

Solar cells can be divided into three different generations; first-generation solar cells are based on silicon materials; second-generation solar cells are thin films, and third-generation solar cells consist of new materials. The efficiency and stability of the first-generation solar cells are good, but they require tough production conditions, such as high temperatures and high vacuum, therefore their fabrication costs are high. The second-generation solar cells have lower costs but also lower efficiencies. The third-generation solar cells have promising prospects.

2.2.1.1 Efficiency and losses

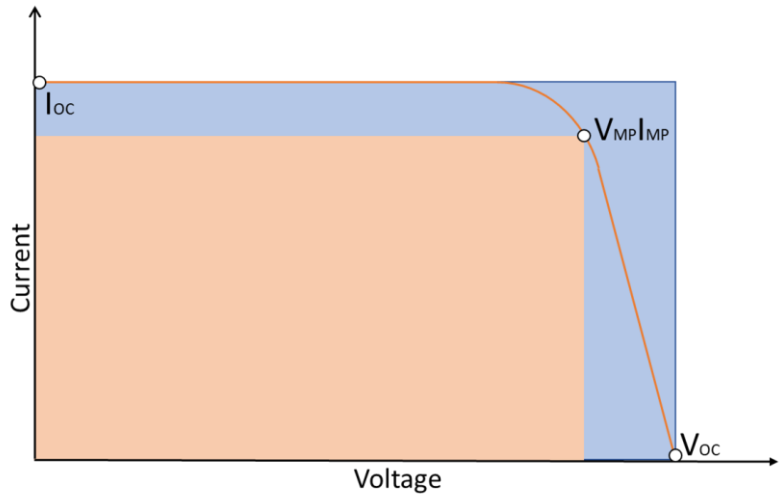

Figure 5. The fill factor, which determines the maximum power from solar cell.

The efficiency of solar cells can be measured using four parameters: short circuit current (i_{SC}), open circuit voltage (V_{OC}), the power entering the panel (P_{IN}, P_{SUN}), and the fill factor (FF). The fill factor is calculated by dividing the multiplication of the maximum power point voltage (V_{MP}) and current (i_{MP}) by the multiplication of the short circuit current and open circuit voltage.

$$FF = \frac{V_{MP} \cdot i_{MP}}{V_{OC} \cdot i_{SC}}$$

$$\eta = \frac{P_{MAX}}{P_{IN}} = \frac{i_{SC} \cdot V_{OC} \cdot FF}{P_{SUN}}$$

The cell efficiency is not to be confused with the panel efficiency. The panel efficiency can be calculated by dividing the nominal power of the panel (P_{NOM}) by the surface area (A) of the panel multiplied by 1000 W/m^2.

$$\eta = \frac{P_{NOM}}{A \cdot 1000 \frac{W}{m^2}}$$

Non-absorption and thermalization, previously discussed, stand out as the primary sources of power loss in solar cells. Additional types of losses include optical losses, such as reflection, transmission, and area loss, and collection losses such as bulk and surface recombination. Reflection losses are caused by interfaces within the cell, and their impact can be mitigated through effective surface design. Techniques such as texturing the front surface, the use of anti-reflection coatings, or light trapping can help minimize these losses. Transmission losses, due to cell thickness, can be addressed by increasing thickness to enhance absorption, although this approach comes with compromises such as higher material consumption and challenges collecting charges from deeper layers. Area losses result from shading by top contacts while bulk recombination refers to the recombination of an excited electron and a hole in the bulk of semiconductors, and the probability of this is affected by the distance of the p-n junction. Surface recombination, which occurs mainly at the front surface, involves recombination of the excited electron at the cell interface or surface. [18]

2.2.2 Silicon solar panels

Silicon solar panels dominate the current global production of solar panels with 90% share of it. There are two different types of silicon solar panels which are mono-crystalline (single-crystalline, mono c-Si, mono-Si) and poly-crystalline (multicrystalline, poly-Si, mc-Si). Mono-Si panels are more efficient since they are made from one piece, and they have high life span, but they are also more expensive. Poly-Si panels are manufactured by casting and it's cheaper to manufacture and they are also more common. Poly-Si on the other hand have lower efficiency and have less uniform look as they have lower purity of silicon.

Silicon solar cells are wafer-based which means that the cells are fabricated on semiconducting wafers, and they can be handled without an additional substrate. Typically, the solar panel modules are covered with protective glass for safety and for mechanical stability. Silicon solar cell's structure consists of three main components: front contact, silicon cell and back contact. The front contact is responsible for the current collection. The silicon cell component is

responsible for the photovoltaic effect and charge separation and the back contact completes the electrical circuit.

Silicon solar cells use only one band gap and are therefore unable to use the entire solar spectrum. William Shockley and Hans J. Queisser calculated in 1961 that the maximum theoretical efficiency of crystalline silicon solar cell would be 30%[19]. This calculation was made by assuming that a single semiconductor and p-n junction constitute a solar cell, without sunlight concentration and that charge carries mobility would be infinite. The solar cell would also be a blackbody so it would absorb all incident radiation [19], [20]. This maximum theoretical efficiency would be achieved at band gap 1.1 eV or ∼1130nm. The maximum theoretical efficiency for silicon solar cell would be ∼33% according to modern version of SQ limit where the thickness is considered, the absorption due to charge carries and auger recombination and the surface of the silicon is optimized (light trapping) [15], [21], [22].

Commercial silicon solar panels have efficiencies of 18-21 % and 15-18% for mono-Si and poly-Si, respectively. The efficiency of solar panels or modules should not be confused with the efficiency of cells, as the efficiency of cells is always higher. There will be small gaps between the panels, resulting in a lower efficiency percentage.

2.2.3 Flexible/thin films panels

Thin film solar cells (TFSCs) constitute a pivotal technology in the solar energy landscape, comprising multiple layers of distinct materials. Among the most widely commercialized TFSC, three stand out prominently: amorphous-silicon (α-Si), cadmium telluride (CdTe), and copper indium gallium selenide (CIGS). These materials offer the advantage of minimum material usage and improving efficiencies, thanks to their direct bandgap properties that enable the utilization of thin materials. Despite their promising features, TFSCs possess a lower absorption coefficient compared to their crystalline counterparts, absorbing less light per thickness. The structure of TFSC is composed of substrate, transparent conducting layer (TCO), window layer, metal contact or back contact layer, and absorber. Every component material has unique physical and chemical characteristics that have an impact on the performance of the cell. [23]

α-Si, a versatile material, finds application on various metallic and non-metallic substrates. Depending on the architecture—whether p-i-n or n-i-p—α-Si cells are deposited onto transparent conductive oxide or fabricated with a glass substrate. The substrate's properties

significantly influence the structural characteristics of the cell. [24] In particular, substrates must remain inert, mechanically stable, and possess a thermal expansion coefficient matching the deposited layers. The use of TCOs, often zinc oxide-based, enhances electrical conductivity and transparency. α-Si cells can incorporate single or double-layer TCOs through microstructure modifications, impacting its overall performance. In amorphous silicon thin-film solar cells, silicon nitride (SiN_x) or a-SiC:H (hydrogenated amorphous silicon carbide) is usually used as the window layer [25]. These provide suitable bandwidth characteristics and optical properties to ensure efficient transmission of light while forming a suitable interface with the absorber layer. The back contact is typically made on an n-type semiconductor layer and a double-layer reflector of ZnO and Ag or Al layers is commonly used. The ZnO layer will enhance the back reflection as well as cell performance due to its optical and electrical characteristics [26].

CdTe, another widely commercialized TFSC material, is often produced in a superstrate configuration, allowing flexibility [27]. The choice of substrate material depends on the deposition temperature, with borosilicate glass or thin metallic foils used for high-temperature deposits and soda-lime glass for lower temperatures. In CdTe thin-film solar cells, these double-layer TCO or bilayers are mostly used. In these bilayers, the properties of two different TCO layers can be combined, and usually one layer is highly conductive, and the other layer is much thinner but highly resistive. Cadmium sulfide has traditionally been used as the window layer material in CdTe thin-film solar cells. Cadmium sulfide has the appropriate bandwidth, good optical transparency and electrical properties needed for efficient performance. However, cadmium sulphide is highly hazardous, so environmentally friendly alternatives such as zinc-based compounds such as ZnS [28], ZnSe [29] or ZnO are constantly being researched, but a fully suitable alternative has not yet been found [30]. Most common and most efficient CdTe solar cells are manufactured by using Cu-based materials as the back contact, but different materials and especially Cu-free materials are searched for all the time [31], [32].

CIGS, a material under active development, exhibits both superstrate and substrate structures. Notably, CIGS cells based on the substrate structure demonstrate superior performance due to the interdiffusion of CdS during high-temperature film growth, contributing to increased solar energy efficiency [25], [33]. These bilayer TCOs are also used in CIGS cells since they are the most functional ones. The CIGS cells also use cadmium sulphide and zinc oxide as the window layer. Molybdenum serves as a commonly used material for back contacts, offering inertness during deposition conditions, high thermal stability, and corrosion resistance. Challenges

persist, particularly under high argon pressure during molybdenum deposition, leading to optical and electrical issues [34].

While α-Si solar cells have dominated the consumer electronics market since the early 1980s, the performance and development of CIGS and CdTe solar cells show promising signs of overcoming crystalline Si technology. Despite this, the thin-film solar cell sector is currently in a slight downturn due to the low manufacturing costs of the corresponding crystalline silicon technology. The expected increase in the market share of thin-film technologies is based on the assumption that production costs will remain lower than those of crystalline silicon. Challenges related to thermal reliability and material availability may affect their role in the growth in demand for PV technology. In addition, cutting-edge thin-film technology based on perovskites is gaining attention thanks to improved stability and reliability. The development of thin film technology balances cost competitiveness with continuous technological development. [23], [25]

2.2.4 Perovskite panels

Among all solar cells used in photovoltaic systems, perovskite solar cells (PSC) had the quickest rate of performance growth with almost 22 percentage points in 13 years [35]. Perovskite is a titanium oxide mineral composed of calcium titanate ($CaTiO_3$) and it was discovered by German mineralogist Gustav Rose in 1839 but it is named after Russian mineralogist Lev Perovski. Perovskite is also referred to all compounds with the same crystal structure as $CaTiO_3$ with the general formula of ABX_3. The A stands for cation, B as metal cation and X for the halogen anion. Perovskite has unique structural properties, tuneable bandgap, high absorption coefficient, high charge carriers' mobility and long electron-hole diffusion length [36].

Perovskite solar cell structure consists of an electrode, hole transporting layer (HTL), perovskite absorber layer, electron transporting layer (ETL) and transparent conductive oxide. The architecture can be regular/standard (n-i-p) or inverted (p-i-n). [37] In regular architecture, the ETL is deposited first on top of the TCO which is usually fluorine-doped tin oxide or indium tin oxide. In inverted architecture, the HTL is deposited first on top on indium tin oxide. The first publication using perovskite materials in solar cell applications was made in 2009. Miyasaka et al. used TiO_2 as ETL and $CH_3NH_3PbI_3$ as absorber layer [38]. Four years later inverted architecture structure was invented [39]. Today, the PCE of a cell made either way is

more than 20%. However, n-i-p type of PSC have the record efficiency for single junction cells [40].

The main operating principle of standard perovskite solar cells consists of three phases. Firstly, the charge generation will occur in perovskite absorber layer. The active material is excited by a photon and creates electron-hole pair. Then the charge separations will occur to the charge selective layers. Finally, the ETL transfers the electrons and block the holes from the perovskite layer to the back contact and the HTL transfers the holes to reach the TCO layers and blocks the electrons. The wire will connect the electrodes creating an external circuit. [41]

Both electron and hole transporting materials (HTM) need to be developed to improve the performance of PSCs even more. For electron transporting materials (ETM) it is necessary to create metal oxides with improved mobilities, fewer surface flaws and better band alignment. Additionally, for flexible and large-scale PSCs, experimenting with various deposition techniques is required to create a suitable metal oxide ETM. The development of organic ETMs is on the rise and looks promising, but there is a lot of work to do in terms of simpler manufacturing methods, higher mobility and durability. [42] Spiro-OMeTAD is the most frequently utilized small molecule for HTMs. However, it has complicated synthesis process and expensive price, so it is necessary to create alternatives with comparable qualities. Stability, simplicity of synthesis, and high purity are desirable attributes. Furthermore, it would be ideal to construct organic HTMs devoid of dopants that exhibit good performance [41].

PSCs have great potential, are developing quickly, and have received a lot of scientific interest in the last ten years. However, problems with commercialization are posed by the coating methods for large area perovskite films, the measurement standards for stability and cell lifetime. In addition, the toxicity of lead and possible solutions to it are also a major concern. [43]

2.2.5 Bifacial panels

An innovative innovation in solar panel design is the bifacial solar panels. Bifacial solar panels are a type of photovoltaic module that can capture sunlight from both the front and back of the panel. Working principal of bifacial panels allows them to produce more electricity than traditional (monofacial) panels. Unlike conventional solar panels that solely absorb sunlight from their front surface, bifacial panels utilize both direct sunlight and reflected light, thereby enhancing their energy output. By converting reflected light, such as that from surrounding

surfaces like the ground or nearby structures, into electricity, bifacial panels leverage what is known as the albedo effect. This is particularly useful in environments with reflective surfaces such as snow, sand, or light-coloured roofs. Studies have shown that bifacial panels can significantly increase energy production, especially in places with high albedo.

Bifacial solar panels offer a promising solution for aligning PV production with fluctuating power demands. In regions like the Nordic countries, where the sun rises early in the east and sets in the west during summer, strategically orienting bifacial panels in a south-north direction can optimize electricity generation to match with peak demand periods in the morning and evening [44].

As the solar industry progresses and technology advances, the popularity of bifacial panels has grown. However, broader acceptance in the global solar market requires a deeper comprehension of the technology, further development of solar cell technology, and establishment of industry standards. To facilitate widespread adoption, efforts must focus on making the technology more accessible and economically appealing [45].

2.2.6 Tandem panels

Tandem solar panels are one the latest inventions in PV industry that are rapidly gaining traction. The fundamental idea behind tandem solar cells is to stack multiple layers of semiconductor materials on top of each other, with each layer optimized to absorb a specific range of wavelengths. Unlike conventional solar cells, which are limited by a single bandwidth, tandem solar cells exceed the limitations imposed by the Shockley-Queisser limit. Tandem solar panels improve efficiency and performance by reducing heat and absorption losses. The use of two different semiconductor materials is not mandatory but is often used to optimize bandgap tunability. [46] This allows a more precise tailoring of the semiconductor characteristics to the solar spectrum. As a result, tandem solar panels are more flexible and efficient in harnessing solar energy over a wider wavelength range.

The tandem solar cells are typically divided into two types: monolithic and multi-junction, also referred to as are two-terminal and four-terminal types, respectively. The main difference between these types is how the semiconductor layers are connected and fabricated. In monolithic solar cells the layers are grown on top of each other in a single, continuous structure and are connected in series. In multi-junction cells the semiconductor layers are however separate and have their own terminals. [46]

The monolithic solar cells require more precise compatibility of materials and efficient charge transport between layer while in multi-junction cells allow more flexibility in choosing materials and optimizing each layer for its specific wavelength range. The monolithic cells are simpler to fabricate as they have continuous structure and can be fabricated similarly to traditional single-junction cells. However, optimization of each layer for specific wavelength range is more challenging. In multijunction cells it's easier to optimize each layer to get broader range of solar spectrum but the fabrication is more complex. In monolithic configurations, the current is limited by the subcell with the lowest current, while the device's total voltage is the sum of its subcells' voltages. In multi-junction configurations, the presence of multiple transparent electrodes can lead to additional reflection and parasitic absorption. Both configurations face challenges related to material compatibility, such as lattice constraints and other properties need to align. [46]–[48]

Most effective tandem solar cells mainly feature a combination of perovskite and silicon, offering efficiencies exceeding 30%. Notably, the record efficiency of 33.9% for dual-junction cells has been achieved in a monolithic configuration. Perovskite has emerged as a prime candidate for the top cell in tandem panels due to its bandgap falling within the range of 1.5-1.7 eV, making it compatible with various materials such as crystalline silicon, CIGS [49], organic [50] and even with itself [51] in both monolithic and multi-junctional configurations [52]. Ongoing research explores tandem solar panels incorporating all organic [53], CIGS/Silicon [54], polymer-CIGS [55] and CIGS/SWCNT (single wall carbon nano tube) cells [56]. Triple junction tandem panels are also being investigated with different materials [57].

The material selection is the most important aspects as each material have different bandgap and properties, which requires the compatibility and suitability of the chosen materials. Tandem solar panels could be used in situations where space is limited and where higher energy production is needed in a limited area. The tandem solar cells have the potential to become cost-effective and scalable for the whole industry.

2.2.7 Building-integrated photovoltaic

Building-integrated photovoltaic (BIPV) is a technology that seamlessly integrates solar power-generating components into building structures. BIPV is intended to be an integral part of the building's envelope as opposed to adding solar panels as an afterthought with a mounting system. This integration not only harnesses solar energy, but also has the dual purpose of contributing to the architectural and aesthetic aspects of the building. There are primarily four

different integration styles or elements for BIPV: roofs, facades, windows and external devices. In roofs, panels can either cover the entire roof or only part of it. In facades, solar panels can be integrated into the outer walls of the building, acting both as a cladding and as an energy generator. The windows can be fitted with transparent solar cells or solar films, thus making them energy-generating surfaces. parapets, balustrades, canopies, or solar shading devices can act as an external device while enhancing the building's energy efficiency and aesthetic appeal. [58]

Different technologies that are utilized in BIPV include solar shingles or tiles, customised solar modules, and solar glass. Solar shingles are designed to resemble traditional roofing materials but contain photovoltaic cells to generate electricity [59]. Customisable solar modules are designed in a way that makes them versatile and can be integrated into various building elements and even for vertical installation. Solar energy glass refers to glass panels designed to collect sunlight and convert it into electricity. These glass panels can be integrated into windows, skylights, and other transparent surfaces. Solar energy glass can take different forms, such as transparent solar cells, solar coatings, or thin-film photovoltaic technologies. The main characteristics of these solar energy glasses include transparency, versatility, aesthetics, and energy efficiency [60]. In addition, a selective solar harvesting window based on transparent photovoltaic and transparent solar absorbers has been developed. This system captures thermal energy for heating interior spaces in winter and reduces indoor cooling needs in summer through vented air circulation [61].

The benefits of BIPV include aesthetics, space utilization, reduced environmental impact and energy efficiency. BIPV enables the design of visually attractive and architecturally integrated solar energy solutions while utilizing the space available on the building surface. Although BIPV systems typically operate at an efficiency of around 15%, they still play a significant role in reducing greenhouse gas emissions by partially meeting the energy demand of the building.

However, BIPV systems also present challenges, in terms of cost, installation complexity, maintenance and efficiency. The initial investment in BIPV systems tends to be higher than for traditional building materials, requiring careful design to integrate them seamlessly, and can complicate maintenance procedures. Despite continuous improvements, the efficiency of BIPV technologies is lower individual solar panels. [58], [62]

2.2.8 Recycling

Implementing the three Rs - reduce, reuse, and recycle - provides a sustainable and environmentally friendly approach to managing end-of-life solar panels. Reducing the materials used in solar panels minimizes the amount of potential waste, while the overall lifetime of the components can be extended by reusing panels and recovering spare parts from other sources. However, when panels reach the end of their life cycle, recycling becomes a necessity. [63] Recycling of solar panels is crucial for the sustainability of the sector, especially given the projected number of end-of-life panels. It is estimated that by 2050, around 80 million tonnes of PV modules will need to be recycled, and by 2030, 8 million tonnes are expected. This figure represents about 10% of the global e-waste expected to be generated during this period [64]. However, current recycling processes are neither adequate nor cost-effective, highlighting the need for more efficient methods to recycle or reuse these panels and materials.

The design of existing photovoltaic panels focuses on longevity and weather resistance, which makes dismantling challenging. These panels are tightly manufactured and consist of different components such as a frame, cover glass, encapsulants, cells, backing plate and junction box. The encapsulants are heated to form a sealing compound, which further increases the difficulty of material recovery. Therefore, optimizing the recycling processes in photovoltaic technology remains a major challenge [65].

Currently, silicon and CdTe panels are recycled using three main methods: mechanical, thermal, and chemical processes. The most frequently applied method is mechanical processes and can be categorized into cutting, peeling, fragmenting treatment, and contactless fragmenting treatment [66]. The main goal of mechanical treatment is to physically separate the materials without causing the encapsulation layers to break. Shredding, crushing, milling, and grinding are all fragmenting treatment methods. The advantages of mechanical processes include the absence of chemicals, low energy consumption, low processing costs and easy access to equipment. However, the processes generate dust and noise, cannot handle toxic substances, and recovering valuable materials with sufficient quality is a challenge.

Heat treatment aims to break down the capsule polymers into volatile molecules, thereby eliminating the adhesive properties of the panel. This degradation occurs at high temperatures by pyrolysis or combustion [67]. Heat treatment allows the collection of very pure materials and the clean separation of solar cells and glass. However, it requires significant energy consumption, involves high investment and operating costs and can produce toxic emissions.

Chemical processing also targets encapsulants and can use organic or inorganic solvents, which can be accelerated by high temperatures or microwaves. Like thermal treatment, chemical processes allow the collection of high-purity valuable materials and the clean separation of solar cells and glass. However, solvents are expensive, polluting and potentially hazardous. In general, thermal, and chemical treatment allow the collection of the higher purity and higher value materials but are more expensive and more environmentally damaging than mechanical treatment [66], [67].

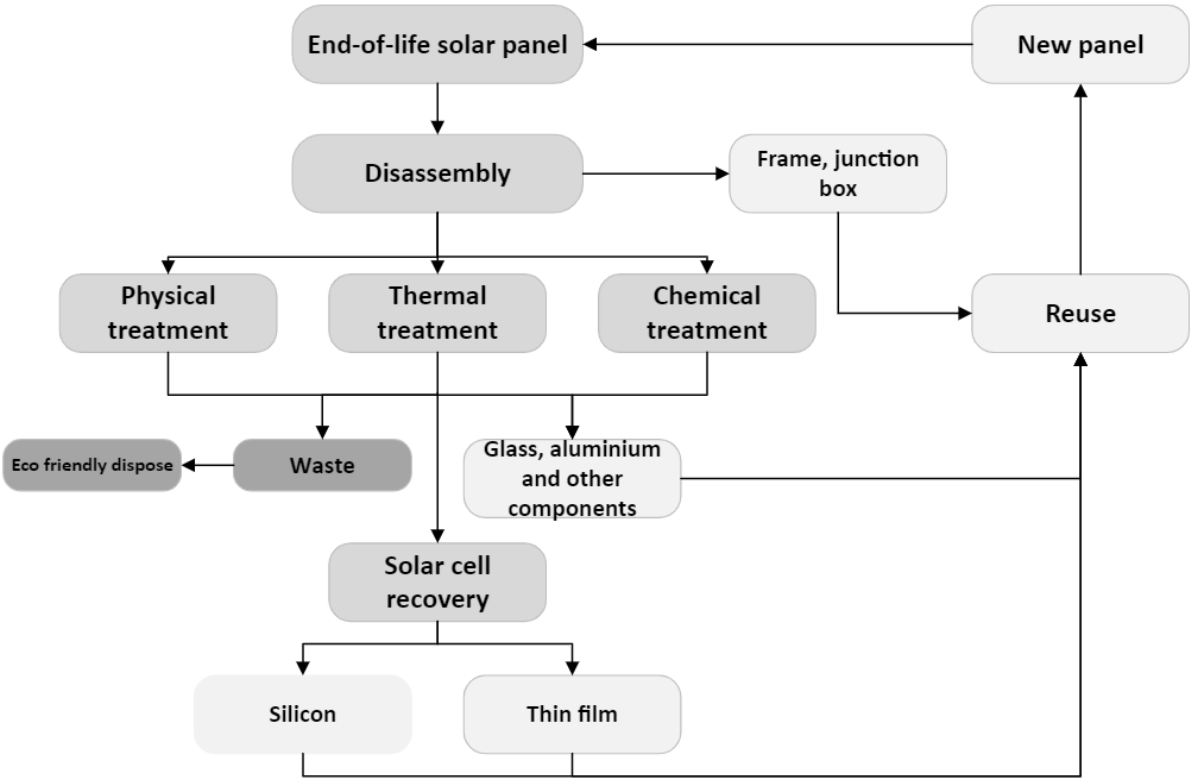

Figure 6. Recycling process of PV panels. Reproduced from refs. [66] and [68] *with permissions from Elsevier and Copyright Clearance Center.*

Majority of the recycling revenue comes from the minority materials by mass such as silver, silicon and copper. However, the purity of these materials significantly impacts their value. Materials must reach high purity levels to be reused in panels; for instance, silicon typically requires a grade of 6N, or 99.9999%. [65] This level of purity is considerably more expensive, approximately eight times the cost of materials with 99% purity [69]. To obtain such high-purity materials from used panels, several EU-funded projects have been initiated. One of the projects aim to develop a recycling plant which could recover up to 98% of the mass of the used

panel with a minimum purity of 98%. One projects goal is to have a plant which will be able to process up to 5 000 tonnes of panels annually by 2023 and the third project concentrates on reusing the waste from wafer production.

Despite these efforts, studies on the economic feasibility of recycling plants give a discouraging message. Recycling plants often struggle to make a profit, as the recycling process often costs more than the revenue generated from the materials [70], [71]. Thus, reusing panels is often more cost-effective than removing components, recycling materials, and buying new ones [72]. An alternative approach could be to redesign PV panels to use more sustainable materials or to make them easier to dismantle [73]. However, such redesign efforts will take time to ensure that the new design matches the efficiency of existing designs.

2.2.9 Sustainability

Compared to conventional fossil fuels like coal and natural gas, solar panels have significantly lower carbon emissions, with reductions of up to 95%. On average, solar panels emits approximately 20-80 g CO_2/kWh, depending on factors such as the panel type and installation method. In contrast, coal emits around 1000 g CO_2/kWh, while natural gas emits around 450 g CO_2/kWh. [74], [75]

The ecological sustainability of solar panels can be assessed through a life cycle assessment, which typically considers measurements of amount of greenhouse gas emissions and energy payback time. Greenhouse gas emissions are measured from product manufacture to the end of the product lifespan and often the recycling is also included to these calculations. In particular, the manufacturing phase accounts for up to 80% of total emissions and includes the extraction of materials, their possible production and processing, and the assembly of the panel itself. While the use of solar panels has minimal environmental impact, emissions from panel transportation contribute to main of the remaining emissions, with variability depending on the location. The energy payback time of solar panels is heavily influenced by solar radiation levels at the installation site. Higher radiation levels result in increased energy production and subsequently shorter payback times. Furthermore, different panel types exhibit varying environmental impacts, with monocrystalline panels generally associated with higher emissions and CdTe thin-film panels with lower. Additionally, installation methods also influence final emissions and payback times. [74], [76], [77]

3 Wind power

Wind energy is actually a second form of renewable energy as it relies on the Sun. As the sun heats the Earth's surface unevenly, the temperature changes, causing pressure differences that ultimately lead to air movement. As warmer air rises and moves towards the poles, cooler and denser air flows over the Earth's surface towards the equator, creating a cycle. This movement of air from high to low pressure areas is commonly referred to as wind [78]. The wind direction is influenced by a number of factors, including the Coriolis effect, pressure differences, local topography, land and sea winds, and global wind patterns. Together, these factors create complex and constantly changing wind patterns worldwide [79]. Thus, certain geographical locations, such as hilltops, mountain valleys and coastal areas, are typically the best places to harness onshore wind energy because of their exposure to prevailing winds.

Harnessing wind energy into electricity through turbine blades is based on the same aerodynamic principles that give lift to the wings of an aeroplane or the blades of a helicopter rotor. As the wind flows over the blades, it creates a low-pressure air pocket underneath each blade, causing motion towards the low-pressure area and starting the rotor spinning. This aerodynamic phenomenon is called lift. The lift force exceeds the wind force in front of the blades, called drag. The combined effect of lift and drag leads to the rotation of the rotor, which is coupled to the generator either directly or through a gearbox. The use of a gearbox allows a physically smaller generator as the gears in the gearbox accelerate the rotation. This rotation converts the aerodynamic force into electricity. Wind turbines therefore convert wind energy into electricity by harnessing the aerodynamic forces acting on the rotor blades. [79]

Wind power is experiencing a significant rise, as illustrated in graph 1, and is poised to become increasingly influential in the near future. Yearly, the cumulative installed wind power capacity continues to grow steadily and providing 2160 TWh of electricity in 2022. This corresponds to 7.6% of global electricity consumption, underlining the growing importance of wind power in the global energy landscape [80].

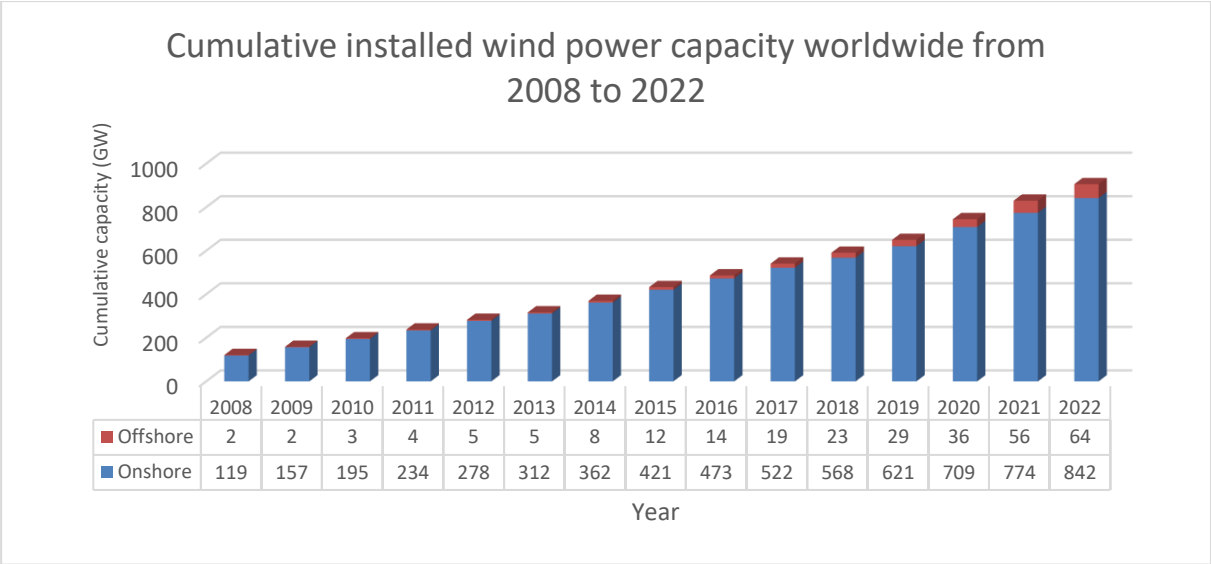

Graph 1. Cumulative installed wind power capacity worldwide from 2008 to 2022 [81].

There are different forms of wind turbines but all of them are categorized distinctly by two types: horizontal-axis wind turbines (HAWTs) and vertical-axis wind turbines (VAWTs). Furthermore, the turbines can be categorized based on their size and capacity to small-scale wind turbines, medium-scale wind turbines and utility-scale wind turbines. The small-scale wind turbines are used in residential or small commercial applications while the medium-scale wind turbines are often used for community or industrial applications. The utility-scale wind turbines are primarily used in specific wind farms for grid-connected power generation. Both HAWTs and VAWTs can be found in small-scale and medium-scale applications, but utility-scale turbines primarily use HAWTs due to their efficiency.

Wind turbines can also be classified based on their working principle, with two primary types: drag-based and lift-based [82]. Drag-based turbines exhibit simplicity in design but tend to have lower efficiency, while lift-based turbines are more intricate, extracting greater energy per unit swept area due to the perpendicular force direction [83], [84]. Advancements in wind turbine technology continue to occur, including innovations in materials, design, and efficiency, making wind energy an increasingly viable and sustainable source of electricity [85].

3.1 Wind turbines

3.1.1 Horizontal-axis wind turbines

Horizontal-axis wind turbines are more traditional in design and to some extent resemble historic windmills. As the name suggests, these turbines feature a horizontal-axis of rotation,

aligning the main rotor shaft parallel to the wind direction. HAWTs are the dominant type of modern wind turbine, commonly found both onshore and offshore, and operate based on lift forces.

The main components for horizontal-axis wind turbine include tower, rotor hub, rotors blades and nacelle. The nacelle includes essential components such as gearbox, main rotor shaft, generator, yaw system and pitch system. Usually, HAWTs consist of two or three blades attached to the rotor hub, capturing the wind's kinetic energy, and converting it into rotational motion. The rotor hub acts as the central connection point for the blades, connecting them to the main rotor shaft, which runs horizontally and is connected to the gearbox. The gearbox increases the rotational speed by using low-speed shaft and high-speed shaft with the generator subsequently converting this rotational energy into electrical power. The generators can be either synchronous or asynchronous generator. The yaw system adjusts the turbine's orientation to face the wind and therefore maximizing energy capture and the pitch system regulates the rotor speed by modifying the blades angle in relation to the wind. The tower supports the entire turbine structure and elevates the rotor to higher altitudes where wind speeds are stronger and more consistent. [85] Tower types can be categorized into five main types: tubular steel towers, Guyed towers, and lattice towers, hybrid towers, and concrete towers. The decision of the tower type is determined by structural, aerodynamic, and budgetary factors [86].

The main differences between a larger scale and smaller scale turbines are the yaw system and the generator. Smaller turbines don't have an active yaw system, but a passive tail that turns the turbine in the winds direction. Smaller turbines also use a direct drive transmission while larger turbines use geared transmission [79].

Another factor influencing the turbine design is the rotor placement which can be either upwind or downwind. The upwind turbines are the most common type, with the rotors facing into the wind and the generator and other components positioned upwind of the tower. In contrast, the rotors of the downwind turbines are facing away from the wind, and the generator is located downwind of the tower. In downwind turbines, the orientation of the rotor means that no yaw system is required.

The advantages of HAWTs include their efficiency, reliability, scalability, and mature technology. Most commercial wind developments worldwide exclusively rely on HAWT due to their superior overall performance, with a typical power coefficient ranging from 40% to 50%. However, challenges such as high maintenance costs, decreased performance in low and

unstable winds, and noise generation hinder their use in urban areas. Despite these challenges, ongoing advancements in technology continue to enhance the efficiency and reliability of HAWTs. As the global demand for sustainable energy solutions increases, HAWTs will likely continue playing a crucial role in harnessing wind power.

3.1.2 Vertical-axis wind turbines

Vertical-axis wind turbines (VAWTs) are a distinctive category of wind turbines, different from the common HAWTs. Unlike their horizontal counterparts, VAWTs have the rotor axis oriented vertically to the ground, which offers both unique advantages and challenges to harnessing wind energy. These turbines are able to generate electricity from winds of any direction, have a low cut-in wind speed and have a design where the main rotor shaft is positioned transversely to the wind, with key components located at the turbine's base.

VAWTs can be categorized into two main groups: the Savonius and the Darrieus models. The Savonius turbine, invented by Finnish engineer Sigurd Savonius in the 1920s, operates based on drag force [87], [88]. It consists of two hollow half cylinders connected to a central rotating shaft, facing opposite directions. While the Savonius turbine doesn’t offer optimal aerodynamic performance, it excels in low wind speed conditions. Over the years, the Savonius turbine has been developed to enhance its efficiency, with advancements in rotor and blade design, blade overlap, and the number of blades. Modern Savonius turbines typically feature a helical design with curved blades forming a symmetrical S-shape. Variations include straight bucket, helical bucket, and multi-stage turbines. These turbines are commonly utilized in smaller-scale applications due to their self-starting design, simple construction, cost-effectiveness, and reliability in low wind speed conditions. However, Savonius turbines face challenges such as limited scalability and lower efficiency rates compared to other VAWTs, with a power coefficient typically only in around 0.20 [84], [89]. Despite these challenges, Savonius turbines remain a viable option for specific applications where low wind speeds prevail.

French engineer G.J.M. Darrieus invented and patented his own design of wind turbine in 1926, though the patent wasn’t granted until 1931 [90]. These turbines, known as Darrieus turbines, are based on the lift force enabling them to extract more energy from the wind per unit swept area compared to Savonius turbines.

There are many different designs of Darrieus turbines, but they all have the same working principle. The blades move forward in a circular path through the air creating a net forward

force due to the relative motion between the wind flow direction and the blade. This forward force generates a positive torque on the rotor, with the only force acting on the blades being tension [91]. The design of Darrieus turbines ensures minimal bending stress on the blades, facilitating the construction of larger-scale turbines [84].

The most well-know Darrieus turbine design is the eggbeater shape (Φ-configuration). It is characterized by two or more curved blades that resemble an eggbeater. Despite its potential for large-scale energy production and having multiple over 100 kW rated turbines, the commercial production has been challenging due to difficulties in manufacturing and high costs [92]. Attempts to improve and optimize the design have not yet delivered significant benefit.

Another Darrieus turbine design is the Giromill, featuring straight blades instead of curved ones. The Giromill may have two or more blades, with two-bladed designs resembling the letter H, also known H-rotor or H-bar design. Variable pitch blades are more effective than fixed ones, potentially addressing starting torque issues, although their construction is complex and reduces profitability and cost-effectiveness for small-scale applications [93].

The Darrieus-Masgrowe turbine, also known as Masgrowe H-rotor, divides the turbine into two levels, each with two or three wings with offset by 90 degrees. While this design may reduce self-starting torque problems, further study is required regarding its feasibility and structural stability, as it has only been tested on small-scale prototypes [84].

One interesting Darrieus variant is twisted or helical three bladed turbine. It is based on computational fluid dynamics simulations and experiments following promising results. The turbine is designed to start in less windy conditions as its twisted blades reduce flow separation providing a positive lift at zero angle of incidence. The twisted blades also can increase the efficiency by increasing the projected area. However, challenges in manufacturing and scalability persist, with the current power coefficient remaining too low for widespread feasibility [93].

One potential solution for vertical-axis wind turbine is a hybrid design of both Savonius and Darrieus turbines. By leveraging both drag and lift forces, this hybrid turbine could offer improved efficiency and self-starting capacity, addressing the shortcomings of each individual design [94]. The hybrid design presents an opportunity to enhance the performance and versatility of VAWTs, potentially increasing their competitiveness in the renewable energy sector.

VAWTs, with their capacity to capture wind from diverse directions, offer simplicity in mounting and maintenance. However, despite their urban suitability and adaptability to complex wind environments, VAWTs are less common in large-scale electricity generation when compared to HAWTs.

3.1.3 Building-integrated wind turbines

Building-integrated wind turbines (BIWTs) are designed to be integrated directly into the architecture of buildings or other structures to capture wind energy and generate electricity. The concept behind building-integrated wind turbines is to make use of available wind resources in urban or suburban environments where traditional wind turbines may not be practical [95], [96]. BIWT can be integrated with four primarily locations: on top of the building, on the side of the building, between the buildings or inside the building.

Despite being in the development phase, notable projects such as The Bahrain World Trade Centre and the Strata SE1 building in London have been completed. However, these projects highlight the importance of careful design when integrating wind energy with buildings.

For example, the Strata SE1 have three 19 kW HAWT integrated on top of the building. While initially projected to generate 50 MWh of electricity annually, these turbines remain inactive due to excessive noise and vibration [97]. In contrast, the Bahrain World Trade Centre successfully integrates three 225 kW HAWTs between its two towers, effectively harnessing wind energy. However, the positioning of the building plays a crucial role, as a different orientation could have resulted in a 14% increase in wind energy production [98].

On the other hand, there are also successful projects, such as The Pearl River Tower in Guangzhou, China. The building features has four VAWT within its structures. The location has very predictable wind patterns and the tower capitalizes on dominant winds from the south or north. Specifically designed openings in the building facilitate wind flow, enabling the turbines to generate an impressive 30,000 kWh of electricity annually [99], [100].

One potential design for BIWT is the Crossflex turbine. The turbine is developed version of the traditional Darrieus vertical-axis wind turbine. The Crossflex turbine features multiple Darrieus turbines stacked within a frame, with the shaft positioned at the ends. Notably, the turbine blades are flexible, enhancing efficiency while minimizing bending stress. Additionally, the absence of blade tips reduces noise emissions. However, the turbine isn’t designed to be scalable, but its modular nature offers potential for deployment in different environments. [101]

3.1.4 Recycling

The recycling the wind turbine face a serious problem as the wind power industry has been growing faster in the last decade. The older generation wind turbines are approaching their end of life and while up to 85% of the turbines mass can be recycled, the main problem is recycling the blades [102]. While the mast, made of steel, is easily recyclable, and the nacelle contains components like gears, generators, and electronics that can be broken down and recycled, the blades pose challenges due to their size and complex composite nature. Turbine blades are typically made from fiberglass-reinforced polymer composites, comprising materials such as polyester resin, epoxy resin, polyvinyl chloride, and fibres like glass and carbon. These blades feature a highly rigid structure and boast a high strength-to-weight ratio [103].

Wind turbine recycling shares similarities with solar panel recycling, utilizing the same three main processes: mechanical, thermal, and chemical treatments. However, the exact processes differ due to variations in component materials between wind turbines and solar panels.

In mechanical treatment, turbine blades are transformed into smaller pieces through cutting methods before undergoing decomposition via grinding, crushing, shredding, and milling. The resulting end product can be separated into resins and fibres, which can then be reused as reinforcing material for concrete. While this approach offers advantages such as high treatment capacity, low cost, and versatility for different materials, it also leads to deterioration of mechanical characteristics and limited opportunities for remanufacturing due to impurities in the end materials [103].

The thermal treatment can be divided into pyrolysis, fluidized bed oxidation and hybrid treatment such as microwaved pyrolysis. In pyrolysis the composite is heated to high temperatures (450-1000°C) in unoxidized space, converting the resin into gas or vapour while the fibres remain inert for retrieval. While pyrolysis offers the advantage of being inexpensive and straightforward, it is sensitive to process parameters and can result in significantly weakened fibre strength. The fluidized bed oxidation involves heating the composites to slightly lower temperatures (450-550°C) in a highly oxidized space, causing the polymer matrices to undergo combustion and separate the fibres. While this method produces high-quality recovered fibres, it suffers from low economic viability, deteriorated mechanical characteristics, and low efficiency [103]. The microwaved pyrolysis uses microwave radiation to break down the resin matrix of composite wastes. The composites internally absorb microwave energy while increasing the rate of disintegration and decreasing processing time

[104]. However, the technique is only at lab scale, so the feasibility and effectiveness remain uncertain at commercial scale [105].

In chemical treatment the fibres are recovered when polymeric resin is broken into oils. The primarily idea is to decompose the polymer matrices to recover both fibres and other degradated products. The solvolysis and the use of subcritical or supercritical fluids are most applied chemical recycling methods. While these methods offer complete segregation of fibres and resins, they generate high costs, are energy-intensive, and have negative environmental impact [103], [105].

Currently, mechanical treatment is the only method operating at a commercial or industrial scale, while thermal and chemical treatments remain at lab or pilot scale. Ongoing research primarily focuses on the microwaved pyrolysis and chemical treatment methods [106], [107].

In addition to recycling, wind turbine parts can also be reused and sold. However, they are typically dismantled and recycled, with recycling costs varying from 10 000 € to 80 000 € depending on turbine size and the number of turbines dismantled simultaneously. Repurposing the site for new wind projects, known as repowering, involves renewing foundations and permits while utilizing existing infrastructure such as electricity wires, roads, and accurate wind data [108].

3.1.5 Sustainability

Wind power can be recognized as one of the cleanest energy sources, having greenhouse gas emissions of around 5-10 g CO_2/kWh for onshore wind power and approximately 15 g CO_2/kWh for offshore wind power [77]. Similar to solar panels, the primary environmental emissions associated with wind power come from the manufacturing process, including the collection of raw materials and the production of turbine components. For onshore turbines, manufacturing phase accounts for approximately 70% of total emissions, whereas for offshore turbines, this share is around 35% [109], [110]. Emissions from starting and assembling the turbine at the chosen location constitute just over 10% for onshore turbines and 25-30% for offshore turbines, with offshore foundation construction being particularly emission and energy intensive. Transport emissions account slightly below 10% for onshore turbines and around 15% for offshore turbines, with variability depending on the location as it affects the construction and transportation.

The energy payback time for wind turbines is notably short, typically half a year up to a year for onshore turbines and slightly longer for offshore turbines. However, this is dependent on the wind speed at the selected location. Moreover, both environmental emissions and energy payback time are influenced by the size of the turbines, with smaller turbines generally exhibiting shorter payback periods and lower emissions. [111] Overall, wind power emerges as a highly favourable energy option with minimal environmental impact and rapid energy payback, particularly when considering advancements in turbine technology and location optimization.

3.2 Emerging technologies

3.2.1 Kite turbines

Kite turbines, also known as airborne wind energy (AWE) systems or airborne wind turbines (AWTs), are unique and innovative approach to harnessing wind energy. Operating as airborne systems, they utilize the movement of a tethered kite to generate electricity. While various designs and configurations exist, the fundamental principle remains consistent, leveraging the wind's force on a tethered flying object to produce power.

The design and structure of kites varies significantly among the companies. Some operate somewhat autonomously, adjusting their position in the sky to optimize energy capture (autonomous kites) and some designs use tethered wings or foils that fly in a circular or figure-eight pattern to generate power (tethered wings or foils) [112]–[114]. Typically, kite turbines consist of a kite or similar airborne structure connected to the ground by a tether. The kite is equipped with turbines or generators that capture the energy as it moves through the air, with the tether transmitting the generated electricity back to the ground.

One of the primary motivations behind the development of kite turbines is their ability to reach higher altitudes where winds are stronger and more consistent compared to ground-level winds. This results in higher energy density and requires less building material compared to conventional wind turbines. Additionally, kite turbine systems can be transported and deployed easily to different locations.

Despite the advantages, kite turbines face significant challenges, particularly related to control, stability, and safety. Effective operation relies heavily on precise control and stability mechanisms to ensure safe and efficient energy generation. Safety concerns also arise due to

the systems operating in airspace, necessitating designs to prevent collisions with other airborne objects [115].

While kite turbines present an exciting and promising concept, they are still in the early stages of development, and challenges related to control, safety, and reliability need to be addressed before they can become widespread. Kite turbines have the potential to for various applications which include off-grid locations, disaster relief and challenging environment. Researchers and companies continue to explore and refine this technology, aiming to unlock its full potential as a viable solution for airborne wind energy generation.

3.2.2 Resonant wind generator

The resonant wind generators exploit a natural phenomenon called vortex shedding. The vortex shedding is a rhythmic pattern of fluid movement that occurs when air or water passes by an object at specific speeds determined by the object's size and shape. This flow generates vortices at the rear of the object, which periodically detach from either side of it [116]. The object starts to oscillate and harness energy when the frequency of the vortexes is the same as the object’s natural resonance frequency.

Company called Vortex Bladeless has been developing this kind of technology with numerous different parties [117]. Their model consists of a fixed base and a cylindrical mast connected by a carbon rod. The mast oscillates freely perpendicular to the wind direction. Inside of the mast is copper coils and on the inner parts of the mast is permanent magnets. Despite the oscillations, internal components avoid collision while generating electricity through electromagnetic induction between the coils and magnetic field. Notably, this technology eliminates the need for a shaft or gearbox. The magnets also serve as a tuning system, adjusting the mast's apparent elasticity and widening the wind speed range for oscillations, thereby enhancing system efficiency [118].

Although still in development, this technology offers compelling advantages such as low maintenance, silent operation, and minimal impact on wildlife. It’s safer, simpler design also promises easier installation and operation. While ongoing development efforts are required before commercialization, the potential of resonant wind generators to diversify wind turbine options and advance wind energy is significant.

4 Energy storage

Energy storages are becoming increasingly important and play a key role in meeting growing energy demand, especially in the context of renewable energy sources. The temporary and variable nature of renewable energy sources, such as solar and wind power, underlines the urgent need for efficient energy storage solutions. Enhancing grid stability, integrating renewable energy, and improving reliability are the main motivations behind the development of energy storages [119].

Energy storage systems operate by capturing and storing surplus electricity generated from renewable sources, such as solar panels or wind turbines, or excess thermal energy. When demand spikes or renewable sources cannot meet power requirements, stored energy is released back into the grid. This dynamic process manages demand variability and the intermittency of renewables, ensuring a steady and reliable electricity supply. The important characteristics of energy storage include the storage capacity, charging and discharging rating power, round trip efficiency, response time, lifetime, reliability, and environmental impact. [120]

Energy storage technologies can be categorized into various types: mechanical (pumped hydro, compressed air energy storage and flywheel), electrical (magnetic superconductors), chemical (hydrogen and power-to-gas), electrochemical (batteries and supercapacitors) and thermal (phase change energy storage). This thesis focuses on three of these technologies: batteries, hydrogen and phase change materials, with each chapter examining their principles, applications, advantages, and associated challenges.

4.1 Battery

Battery storage technology is essential in the renewable energy sector, mitigating the intermittency of sources like solar and wind power by storing electrical energy for later use. Batteries are divided into two categories based on their chargeability: primary and secondary batteries. Primary batteries can release stored energy only once, such as basic alkaline batteries which are found in a lot of household appliances, whereas secondary batteries can be discharged and recharged multiple times.

The battery is essentially composed of five different components: cathode, anode, separator, enclosure, and electrolyte. The cathode and anode constitute the positive and negative sides of the cell, respectively, with a separator positioned between them to prevent short circuits. The

enclosure, also known as the battery casing or housing, serves as the protective outer shell that contains and protects the internal components of a battery. Lastly, the electrolyte facilitates the flow of electric current by enabling the transport of ions between the anode and the cathode. [121], [122]

The battery storage working principle is based on a redox (reduction-oxidation) reaction. The oxidation occurs in the anode electrode, and it releases electrons into the external circuit and forms positive ions during the electrochemical reaction. The reduction occurs in the cathode and the electrons from the external circuit combine with positive ions. During discharge, electrons flow from the anode to the cathode through an external circuit, while ions move internally from the anode to the cathode through the electrolyte. This creates a potential difference between the anode and the cathode, allowing electrons to flow and creating an electric current. During charging, the external electrical supply forces the electrons to be released from the cathode to the anode, while the ions move from the cathode to the anode through the electrolyte. [123]

The external energy is therefore stored in the battery as chemical energy in the anode and cathode materials, which have different chemical potentials. The choice of electrode materials directly affects the cell voltage, as by calculating the Gibbs free energy change of the overall electrochemical reaction, the theoretical battery voltage can be obtained. Battery cells are combined into packs to achieve higher voltage and capacity, with cells connected either in parallel or in series [124].

Battery storage systems offer numerous advantages in the field of energy management: They contribute to grid stability by providing a buffer against variations in supply and demand, thus enabling a more reliable and stable electricity supply. They also facilitate the integration of renewable energy sources. Another benefit of battery storage is its ability to provide backup power in emergency situations, which increases the resilience of the grid and ensures continuous power supply to critical facilities or during power outages. Battery storage systems also help manage peak loads by discharging stored energy during periods of high demand, reducing the strain on the grid and potentially lowering electricity costs.

While battery storage systems are scalable and allow for tailoring to specific storage needs, increasing storage capacity usually requires increasing the number of cells, which can increase physical size, costs, and system complexity. However, continued advances in battery technology, such as the development of lithium-ion batteries, sodium-ion batteries and flow

batteries, are aimed at improving efficiency, reducing costs and improving overall performance, making battery storage an increasingly viable solution for energy management and storage [119].

4.1.1 Lithium

A lithium-ion (Li-ion) battery is a secondary type of battery that has become one of the most widely used energy storage technologies in various applications, from consumer electronics to electric vehicles and renewable energy systems. It has gained popularity due to its high energy density, relatively light weight, and ability to hold a charge for an extended period.

Like many other battery chemistries, Li-ion batteries need anodes and cathodes that conduct electricity and ions to work. They also need electrolytes and separators that are electrically insulating but ionically conductive. The working principle of Li-ion battery is the same as described in previous chapter. The lithium-ions move between the cathode and anode via electrolyte during charging and discharging cycles, while the electrons move in the external circuit. [123]

Various combinations of materials are used in Li-ion cells to optimize performance and characteristics. Three primary types of cathodes are layered transition-metal oxides, spinels, and olivines. Layer oxides as lithium cobalt oxide ($LiCoO_2$) has often highest capacity but also cost and safety concerns. Spinels as lithium manganese oxide ($LiMn_2O_4$) can reach high power densities with lower cost and safety disadvantages but can be affected by poor electronic conductivity and structural stability problems. Olivines as lithium iron phosphate ($LiFePO_4$) has much better safety and cycle life than its counterparts. However, it also has much smaller holding capacity and specific energy [121], [122].

The development of anodes has been severely overshadowed in recent times, as the development of lithium batteries has been limited by cathode materials. Anodes are cheaper, more stable and have a higher specific capacity. Currently, carbon-based materials such as graphite and hard carbon are primarily used as anodes, but lithium titanate spinel structure is also an alternative.

The electrolyte typically consists of a mixture of organic solvents containing a dissolved lithium salt, such as lithium hexafluorophosphate ($LiPF_6$). However, safety concerns related to electrolyte stability and flammability remain significant challenges. Several options as non-

flammable electrolyte additives, inorganic electrolytes, and solid or polymer electrolytes are being developed but none has yet been proven to be successful [122].

Lithium-ion batteries offer several advantages, including high energy density, relatively low self-discharge rate, high efficiency, wide application range and lack of the memory effect. However, they also face challenges, regarding their relatively high price and potential safety concerns, particularly if the battery is damaged or subjected to extreme conditions. Continuous research and development aim to improve the performance, safety, and cost-effectiveness of lithium-ion batteries for various applications.

4.1.2 Sodium-ion

A sodium-ion (Na-ion) battery is a secondary type of battery that has attracted attention as an alternative to lithium-ion batteries, primarily due to the abundance of sodium salts, making them a potentially cost-effective and sustainable alternative. While research into sodium-ion batteries began in the 1980s, the developments in lithium-ion batteries diverted attention elsewhere [125]. However, the interest in sodium-ion batteries recovered in the 2000s and since 2010s the developments has been rapid, but research is still largely in laboratories and there are only few products on the market [126].

The structure and working principle of sodium-ion batteries closely resemble those of lithium-ion batteries, comprising anodes, cathodes, electrolytes, separators, and enclosures. During discharge, the sodium ions are extracted from the anode material and move to the cathode through the electrolyte. The electrons move from the anode to the cathode via an external circuit generating current. In charging the external power applies voltage to the battery which causes the detachment of sodium ions from the cathode material. The sodium ions move via electrolyte to the anode and at the same time, the electrons move from the cathode to the anode through the external circuit.

Despite similarities, sodium-ion batteries exhibit differences in characteristics due to the elemental disparities between sodium and lithium. Sodium's higher relative atomic mass, ion radius, and redox potential enable its use in electrolyte solvents, salts, and separators. However, these factors also result in lower theoretical capacity, slower reaction kinetics, and increased risk of structural collapse during the electrochemical cycle compared to lithium-ion batteries [125].

The cathode materials control the capacity of the batteries since their theoretical specific capacity is low. The anode influences the reaction's kinetic performance, and the electrolyte influences the stability and safety of the batteries. The cathode materials can be divided into two groups: layered materials, such as Sodium cobalt oxide (Na_xCoO_2), and open-structure materials [127]. The layered materials can have anion-dense or quasi-dense structure. The open-structure materials can be divided into polyanionic compounds, such as sodium iron phosphate, and metal-organic compounds, such as Prussian blue and its analogs [128]. The layered materials have larger energy storage per unit volume, but the open-structure materials are cheaper. A commercially suitable anode material has not yet been found, but different materials such as hard carbon and various titanates are being developed. The electrolyte typically comprises sodium salt, solvent, and additives. Key properties of a good electrolyte include thermal and chemical stability, a wide electrochemical window, and high ionic conductivity. Glass fibre is commonly used as a separator due to its compatibility with the electrolyte, but it has mediocre mechanical properties [126].

Overall, sodium-ion batteries have the potential to be a large-scale stationary energy storage system for renewable energy grids. Their advantages include low cost, abundance of raw materials, high recyclability, and safety. These factors make them well-suited for the next generation of large-scale energy storage solutions. However, ongoing research efforts should prioritise improving various aspects of sodium-ion batteries, particularly focusing on addressing challenges related to the electrode-electrolyte interface and mitigating the risk of structural collapse during the redox reaction. By enhancing performance, extending the life cycle, ensuring safety, and improving charging and discharging rates, sodium-ion batteries can become more competitive in the market, ultimately accelerating their commercialization and widespread adoption.

4.1.3 Flow battery

Flow batteries, also known as redox flow batteries, are a type of secondary battery system that stores energy in liquid electrolyte solutions contained in external tanks. Unlike traditional batteries, flow batteries utilize liquid electrolytes instead of solid electrodes for energy storage. The key components of a flow battery include electrolyte tanks, a cell stack, pumps, and ion-selective membranes [129].

The electrolyte tanks hold different electrolyte solutions called anolyte and catholyte, which flow through the anode and cathode, respectively. The cell stack, consisting of several cells

connected in series or parallel, converts energy. Pumps circulate the electrolytes to the stack, where the ion-selective membrane separates the solutions, preventing short circuits. During discharge, the anolyte undergoes oxidation at the porous electrode, producing electrons that travel to the cathode through an external circuit, where reduction takes place. Continuous flow is maintained by circulating both solutions between their storage tanks. The power rating depends on the number of cells and electrode surface area in the cell stack, while the energy capacity is determined by the size of the electrolyte tanks [130], [131].

The choice of electrode and electrolyte materials is crucial for flow batteries. The flow battery's corrosive environment restricts the possible electrode materials. The electrode should have a high porosity, surface area, and electrochemical stability as well as small electronic resistance. Common materials include carbon-based substances like graphite, though research constantly explores alternatives like metal oxides. The electrolyte affects the overall effectiveness of the battery, and the flow batteries are often categorized by the used electrolytes such as vanadium, zinc-bromine, or iron-chromium. The aqueous flow batteries are most studied as they are cost-effective, easy and are not flammable or explosive. However, the voltage is limited by the electrochemical potential window of water. Organic solvents and ionic liquids are being developed to overcome this limitation. Nevertheless, they tend to be expensive, prone to combustion, volatile and exhibit limited conductivity. One other option is hybrid-flow batteries which can deposit and dissolve materials at one or both electrodes leading to higher energy density. The most common aqueous electrolyte used is vanadium and the most common hybrid is zinc-bromine. [130]

Flow batteries offer flexibility, long cycle life, safety, power independent of the energy capacity and low self-discharge rates, making them suitable for grid energy storage and renewable energy integration. The safety and the decoupled power and energy are the most relevant advantages. This allows the high flexibility, and they can be easily customised to suit different applications in terms of response time, such as designing for fast power distribution or longer-term energy storage [131]. However, their limitations include high price and low specific and volumetric energy [132]. Developing a high energy and power density system while reducing costs is crucial for their widespread adoption.

4.2 Hydrogen

Hydrogen energy storage plays a pivotal role in addressing the intermittent nature of renewable energy sources, providing a reliable means to store excess energy generated during peak production periods. The versatility of hydrogen as an energy carrier extends beyond electricity generation as it can serve as a clean fuel for various sectors, including transportation and industry, and helping to reduce greenhouse gas emissions. However, the production of hydrogen is necessary to obtain it as it is highly uncommon in the Earth's atmosphere and practically absent as a free molecule (H_2) on the surface or underground [133]. There are several methods for producing hydrogen, including steam methane reforming, electrolysis, direct solar water splitting, and biological processes. Steam methane reforming is the most common industrial method. The methane (CH_4) reacts with steam (H_2O) producing hydrogen and carbon monoxide.

$$CH_4 + H_2O \Rightarrow CO + 3\ H_2$$

The rest is produced by electrolysis. In electrolysis, the water (H_2O) is split into hydrogen (H_2) and oxygen (O_2) using electricity.

$$2\ H_2O \Rightarrow 2\ H_2 + O_2$$

Direct solar water splitting involves using semiconductors to harness solar energy and for the electrolysis of water, splitting it into hydrogen and oxygen. Biological processes, on the other hand, involve certain microorganisms, like algae, which can produce hydrogen through photosynthesis, offering a natural method for hydrogen production.

Once the hydrogen is produced it can be stored in various ways. The large divide is between physically or via another material. Physically it can be stored as compressed gas, cryogenic liquid, or cryo-compressed hydrogen. Through another material it can be stored by chemical sorption or physical sorption. Chemical sorption involves storing hydrogen within solids, forming metal hydrides, such as magnesium-based or complex hydrides while in physical sorption the hydrogen is stored on the surfaces of solids, such as carbon structures, zeolites or organic polymers.

Storing hydrogen as gas or liquid requires high pressure or low temperatures due to its low-density mass (0.089 kg/m^3). Compressed gas storage is the most common method, requiring pressures between 350 and 800 bars. The storage vessels are commonly made from steel and

aluminium but also carbon fibre is used to reinforce the vessel [134]. Another method for storing hydrogen as gas is in underground caverns. These caverns can be filled with hydrogen during periods of excess energy production and released during times of high energy demand [135].

Cryo-compressed hydrogen storage combines aspects of gas and liquid storage but is affected by heat loss and energy consumption during liquefaction.Liquid hydrogen storage allows for higher energy density but requires cryogenic temperatures and causes energy losses during liquefaction [136]. Cryo-compressed hydrogen storage combines aspects of gas and liquid storage but is affected by heat loss and energy consumption during liquefaction. The hydrogen is compressed at cryogenic temperatures which has a higher storage density than either of the systems as individuals [137].

Each storage method has its advantages and challenges. Solid state storage system has potential to be one of the most feasible hydrogen storage systems but face challenges in storing and releasing large quantities at low temperatures [135]. Underground caverns offer large storage capacity, with fast response time and multi-purpose use but require suitable geological conditions [138]. Vessel storage achieves high energy densities but faces challenges in material compatibility and energy consumption [134]. Liquid hydrogen storage offers higher energy densities but suffers from energy losses during liquefaction [136]. Overall, hydrogen energy storage systems act as a critical enabler for the widespread adoption of renewable energy, offering a sustainable solution to the challenges of grid reliability and energy demand fluctuations.

4.3 Phase change energy storage

Phase change energy storage or latent heat storage, is a highly efficient method for storing thermal energy, offering high energy densities and effective energy release during phase changes. This technology involves utilizing phase change materials (PCMs) that transition between solid and liquid states to store and release thermal energy. The transformation is also known as melting-solidification cycle [139].

During the charging process, thermal energy is added to the system, causing the PCM to transition from solid to liquid. Conversely, during the discharge process, the stored energy is released as the PCM transitions back to its solid state [140]. PCMs are selected based on their

compatibility with the desired application scenario and offer a suitable, affordable, and effective solution for thermal energy storage.

There are various types of PCMs, including organic, inorganic, and eutectic materials, each with distinct properties and working temperatures. The organic materials can be divided into paraffins and non-paraffins. The inorganic materials can be divided into salt hydrates and metallics and the eutectics are a combination of two or more organic and inorganic materials. [141]

The desired properties include high thermal conductivity, high density, non-corrosive, cost effective and availability. The paraffins are chemically stable, have a high heat of fusion and have good availability but are costly and have low thermal conductivity. The non-paraffins are mainly fatty acids and have similar properties as paraffins with have better phase transitions but are mildly corrosive. The salt hydrates have high thermal conductivity, high density, and good availability but are corrosive and have a high degree of supercooling. Supercooling is a phenomenon where a liquid remains in a liquid state even though its temperature is below its normal freezing point. The metallics consist of metal alloys and metal eutectics. They offer advantages such as high heat storage capacity per unit volume and good thermal conductivity. However, they can be costly to produce and have a lower heat storage capacity per unit weight [141], [142].

Phase change materials find applications in building applications [143], [144], solar energy storage [145], [146], temperature control in electronics and electric vehicles [147]. In building applications, the phase change materials can be embedded into building materials where they can absorb surplus heat during the day and release it during cooler periods while contributing to the energy efficiency. In solar energy systems the PCMs can absorb and store the heat energy for later use and in electronics and electric vehicles, PCMs can be utilized to control the temperature preventing overheating and improving efficiency.

Energy storage based on PCMs is an interesting and promising technology for managing thermal energy effectively in various applications, but challenges remain, particularly regarding operating temperature ranges and material compatibility. Ongoing research focuses on developing new and improved materials, optimizing performance, and expanding the range of applications for phase change energy storage technology.

5 Case study

5.1 Site analysis

5.1.1 Consumption profile

To assess the potential of a renewable energy system, it's crucial to understand the electricity consumption patterns. Graph 2 provides an overview of the average electricity consumption per hour, showing variations on a monthly and yearly basis.

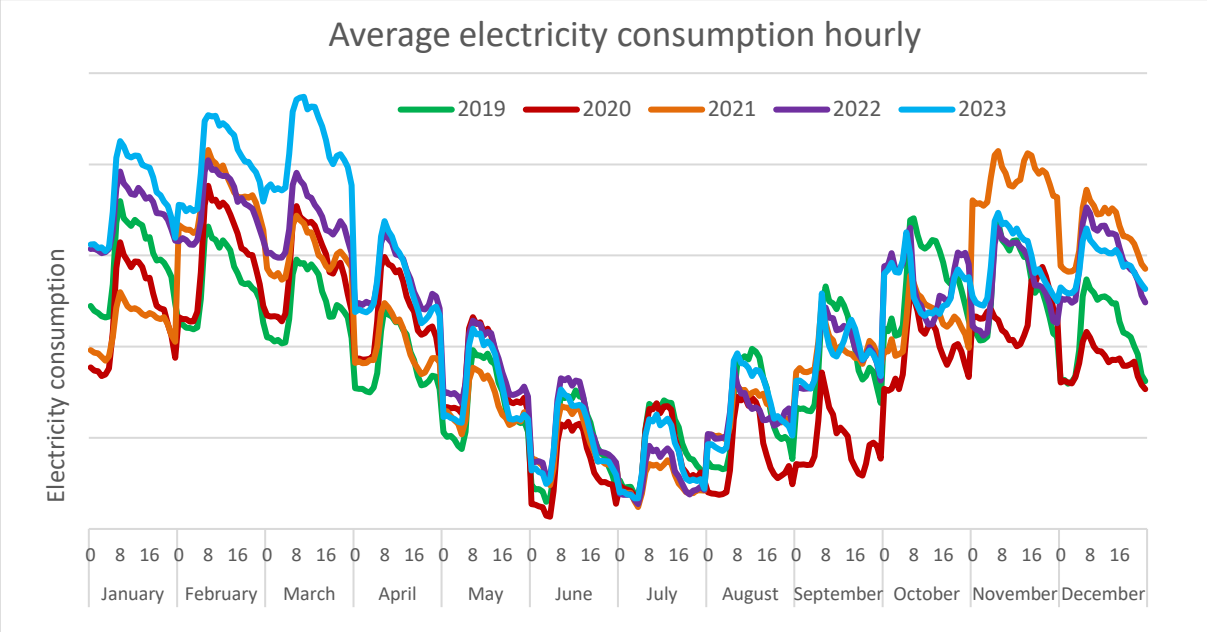

Graph 2. Average electricity consumption hourly [148].

The average consumption profile chart reveals significant seasonal variations, with electricity consumption peaking during the winter months compared to the summer months. Additionally, there are noticeable consumption spikes around 8 o'clock which is followed by a slight decrease in consumption during the working day. Another slight spike in consumption is observed around 17 o'clock and after this peak, consumption drops significantly and remains relatively stable throughout the nighttime hours. It's important to note that this chart represents the average of hours throughout the month, so weekend hours also contribute to the averages.

Furthermore, graph 3 illustrates two typical work weeks during the year, one in January and another in July. The daily consumption profiles are similar to those in graph 2, but with decreased consumption levels on weekends, falling even below the nighttime levels of

weekdays. This analysis helps define the base load and provides valuable insights for assessing the potential of renewable energy systems.

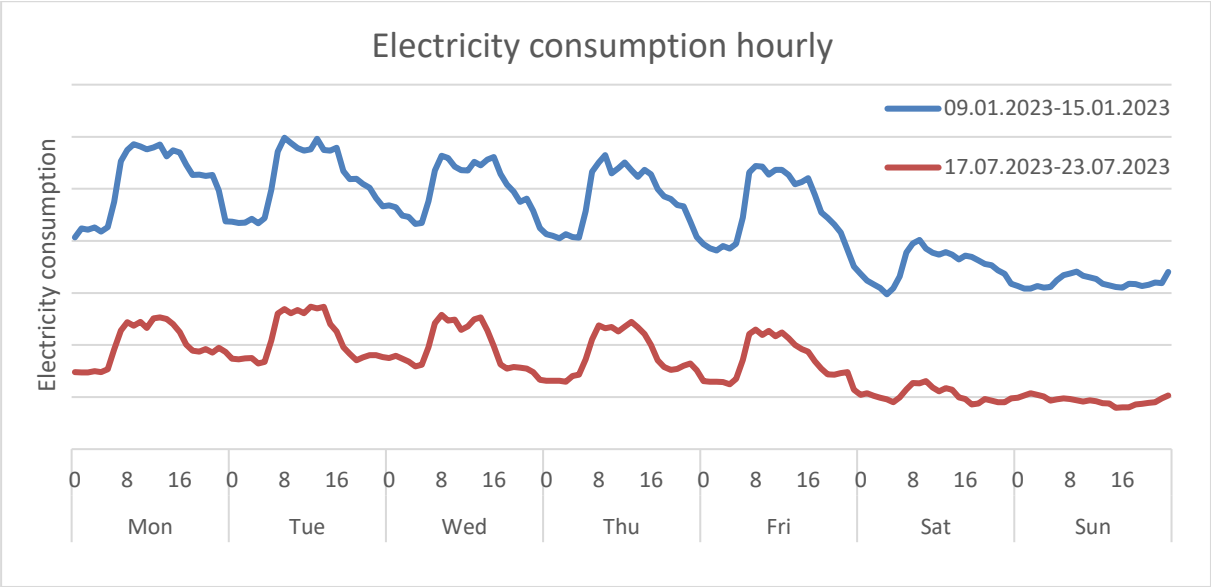

Graph 3. Electricity consumption hourly [148].

The base load refers to the minimum level of electricity demand that is consistently maintained over time, representing the constant need for electricity. Understanding the base load is crucial for designing energy systems and determining the extent of self-sufficiency without the need for energy storage. Typically, the base load occurs during periods of low demand, such as nighttime or weekends. As illustrated in graph 2 and 3, the base load varies throughout the year, with higher base loads observed during the winter months compared to the maximum consumption levels in the summers. This variation reflects seasonal changes in energy demand due to factors such as heating requirements during colder months. The annual baseload is therefore the minimum consumption during the minimum period. This information provides valuable insights for sizing renewable energy systems and optimizing energy production to meet base load requirements efficiently.

5.1.2 Location

The area of Meyer Turku property is over 1 km^2 and is located on the border of Turku and Raisio, in the neighbourhood of Perno. The nearest residential area in the east is less than a kilometre away as well as in the north, and the headquarters of the Coastal Fleet is nearby in the southeast.

Figure 7. Area of Meyer Turku, red lines represent property boundaries. Copyright (2024) under CC BY 4.0 license from ref. [149].

5.2 Electricity price

The price of the electricity is also an important aspect of the design renewable energy system.

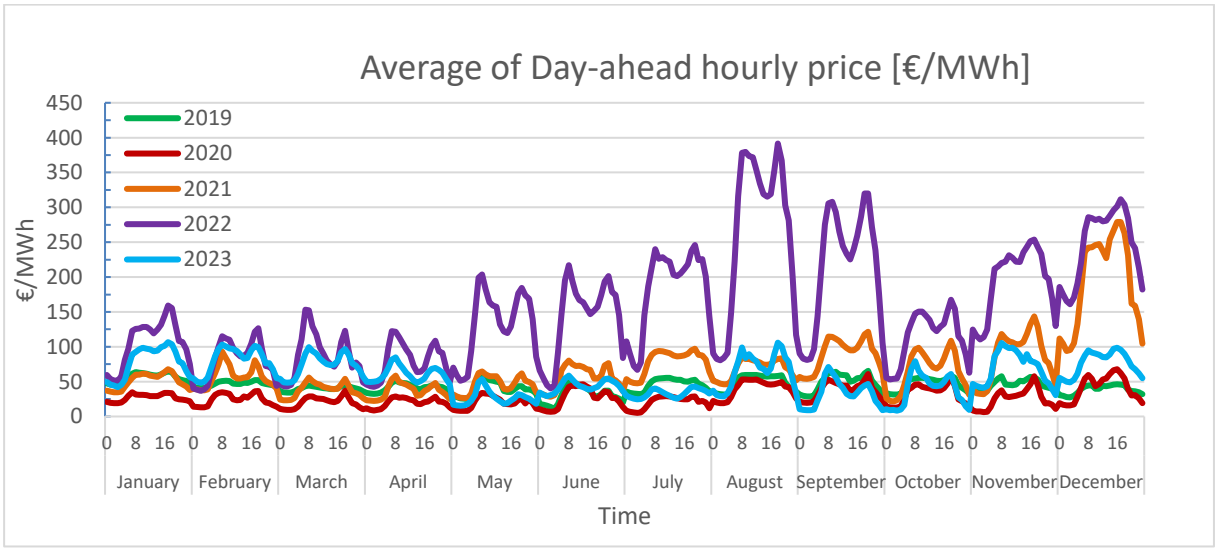

Graph 4. Average of Day-ahead hourly prices [€/MWh] during years 2019-2023 [150].

From the graph 4 can be seen the average Day-ahead prices from years 2019-2023. The figure describes the hourly and seasonal variation. Typically, there are two price spikes during the day, in the mornings around 8 o'clock and in the afternoon around 17 o'clock. Prices tend to decrease between these spikes before dropping in the evening. The yearly variation is

significant, with a notable "energy crisis" between the end of 2021 and 2022, resulting in substantially higher prices. Prior to and after the crisis, prices ranged from 50 to 100 €/MWh (5-10 cents/kWh), while during the crisis, averages reached around 300 €/MWh (30 cents/kWh). These values are tax-free, although Finland imposes a 24% electricity tax, except for a period from December 1st, 2022, to April 30th, 2023, when the tax was reduced to 10% due to rising electricity prices [151].

The total price of electricity in Finland comprises three components: the price of electrical energy, the network service charge, and electricity tax (including the security of supply fee), plus VAT [152]. While taxes and network service charges are fixed, the price of electrical energy can be controlled. It can either be fixed price, ensuring consistency or then day-ahead price where the price fluctuates hourly.

The network service costs include both fixed charges and electricity transmission costs, with the latter varying throughout the year. During winter weekdays (November 1st to March 31st, Monday to Saturday, 7 o'clock to 22 o'clock), the charge is 1.13 cents/kWh (VAT 0%), while for the rest of the time, it's 0.454 cents/kWh (VAT 0%). The level of electricity taxes depends on the usage category, with the industry falling into the reduced tax category 2, resulting in a rate of only 0.063 cents/kWh (VAT 0%). [153]

This information is valuable for assessing the feasibility of a renewable energy system since it allows for more accurate calculations. When electricity is self-produced, transmission costs can be disregarded, reducing the overall expenses. Additionally, the fixed basic charge imposed by the local electricity network company, Turku Energia, remains constant regardless of electricity consumption and should therefore be excluded from the calculations.

For solar power, since most of the production occurs outside of wintertime (about 4% of the yearly solar power is produced during wintertime), the transmission fee is a weighted average of the regular transmission fee and the winter transmission fee. This weighted average is calculated based on the proportion of solar power generated during each period, resulting in a yearly transmission fee of 0.481 cents/kWh (VAT 0%).

For wind power, the calculation is a bit more complex. By dividing the sum of wind power generation during wintertime by the sum of wind power generation throughout the year, the percentage of wind power generated during wintertime can be determined. With this percentage (24% in this case), the weighted average of transmission fee can be calculated for wind power,

which results in 0.616 cents/kWh (VAT 0%) for the yearly calculations. These calculations allow for a more accurate assessment of the savings achieved by producing energy from solar and wind sources compared to relying on grid transmission.

For electricity produced for own use, it must still be taxed, but at a lower rate. During winter days (December 1st to end of February, Monday to Friday, 7 o'clock to 21 o'clock), the tax rate is 0.896 cents/kWh (VAT 0%), and for other times, it is 0.255 cents/kWh (VAT 0%) [153]. For solar power, since only 1% of the yearly potential solar energy is produced during winter days, the weighted average tax rate is calculated accordingly, resulting in 0.261 cents/kWh (VAT 0%).

For wind power, the percentage of power generated during winter days is determined by dividing the sum of wintertime wind power generation by the sum of wind power generation throughout the year. With this percentage (12% in this case), the weighted average tax rate for wind power is calculated to be 0.332 cents/kWh (VAT 0%) for the yearly calculations. These calculations provide insight into the tax implications for producing energy for own use from solar and wind sources during different periods of the year.

When assessing the profitability and payback duration of solar and wind power systems, it's vital to consider these factors in the calculations. Essentially, the calculations contrast the benefits of producing one's own energy with the cost of purchasing energy from the grid. This involves using a fixed and/or Day-ahead price as a reference point. Revenues are multiplied by this price (z), to which the transmission and electricity tax is added, and then the tax on self-generated electricity is subtracted.

Predicting price fluctuations is challenging, and numerous factors influence them, including the number and power of systems. According to the Finnish grid operator Fingrid [154], Finland could have seven gigawatts of solar power in operation by 2030 and according to Finnish Wind Power Association and Sweco, there are 404 wind power projects in the pre-screening or design phase with a combined capacity of 134 453 MW by the end of 2023 [155]. According to Motiva, a state-owned sustainable development company at the end of 2023, Finland had a total of 1 601 operational wind turbines with a capacity of 6 949 MW, which corresponded 18% of Finland's electricity consumption in 2023 [156]. Additionally, the Energy Agency, an expert agency under the Ministry of Economic Affairs and Employment, estimated that by the end of 2022, approximately 635 MW of solar power generation capacity had been connected to the electricity grid, which corresponded 0.6% of Finland's energy production in 2022 [157]. This

represents a significant increase in energy production, and the full extent of its effects remains uncertain.

5.3 Production profile

5.3.1 Solar power

Currently, Meyer Turku has a 546.5 kWp solar system installed on the roof of a warehouse [148]. The rated output of a solar panel, known as Wp or watt peak, indicates its maximum power output under standard conditions of 25 °C solar cell temperature and 1 000 W/m^2 solar irradiance. However, the panel can produce more or less than the rated output based on the irradiance. In southern Finland, a 1 kWp solar system typically generates between 800-1000 kWh of electricity annually, depending on factors like orientation, slope, temperature, and overall system efficiency [158].

The current solar system consists of 1584 modules, each with a power rating of 345 Wp and dimensions of 1956 × 992 mm. There are eight inverters with a total power capacity of 860 kW. The panels are oriented to an azimuth angle of 0 degrees and a slope of 20 degrees, with 40 cm spacing between modules. The system occupies 6500 m^2 of space on a roof that is 7600 m^2 in total implying that the whole roof space is fully utilized by the existing solar panel system.

The current solar panel system produces around 450 000 kWh annually, but its efficiency is lower than expected, with the potential to generate 550 000 kWh per year according to photovoltaic geographical information system, PVGIS [3]. The overall losses amount to almost 34%, which is significantly higher than typical losses for a solar panel system. Notably is good to remember that every system will produce less than its fully potential.

The energy output of the panel can be calculated with irradiance:

$$E = GHI \cdot A \cdot \eta \cdot (1 - X)$$

where, GHI is the global horizontal irradiance which is the total short-wave irradiance received by a surface horizontal to the earth's surface, including both direct normal irradiation and diffused horizontal radiation. A indicates the area of the panel, while η represent the efficiency of the panel. The variable X includes system losses due to inverters, wiring, reflection, shading, and temperature. It's worth noting that temperature plays a significant role in determining the extent of temperature loss. Additionally, the orientation and slope of the panels have a considerable influence on the amount of irradiance received.

The azimuth, or orientation, represents the angle of the PV modules relative to the direction due South. A value of -90° indicates East, 0° corresponds to South, and 90° signifies West. Slope refers to the angle of the PV modules from the horizontal plane, typically for a fixed (non-tracking) mounting configuration. Irradiance data is sourced from PVGIS with database ERA 5 [3], a free web application provided by the EU that offers information on solar radiation and photovoltaic system energy production across many regions worldwide.

According to PVGIS - ERA 5, the optimal azimuth angle and slope for achieving the highest yearly irradiation in Meyer Turku are 46° azimuth and 2° slope, resulting in an irradiation of 1347 kWh/m^2. Comparatively, the difference in yearly irradiation between this optimal combination and, for instance, azimuth 25° and slope 20° is approximately 9%.

Table 1. Irradiation (kWh/m^2) in Turku with different slopes and orientations [3].

Slope / Azimuth	10°	20°	30°	40°	45°
-90°	1040	1026	1012	991	977
-45°	1125	1184	1226	1244	1243
-25°	1149	1228	1282	1310	1312
0°	1160	1249	1311	1344	1347
25°	1151	1233	1290	1319	1322
45°	1129	1193	1238	1259	1259
90°	1046	1038	1028	1010	997

However, optimizing for the highest yearly irradiation may not always be the most desirable approach. In Turku, solar elevation angles are positive for 50% of the year, with an average of 21°. This means that to accommodate multiple rows of solar panels on a flat surface, significant gaps between the rows would be necessary to prevent shading. However, with a slope of 10° or 20°, the required spacing would be smaller.

Aligning solar panel production with consumption is crucial for maximizing profits. Given the significant consumption in Meyer, this factor can be de-emphasised. Additionally, Day-ahead prices fluctuate throughout the day and are influenced by the overall production and consumption. For instance, if everyone orients their panels at azimuth 0°, solar energy production would be high, leading to a decrease in electricity market prices and potentially

reducing profits. Therefore, maximizing overall production is not the sole consideration when designing a suitable PV system.

Various factors must be considered during PV system design, including the electricity and PV system prices, which are often influenced by system power and efficiency, as well as energy losses. As discussed in previous chapter the future electricity prices are difficult to forecast as the production will increase significantly. Swanson's Law offers a formula for forecasting solar panel prices. According to this law, the price of solar panels decreases by 20% each time the cumulative capacity of solar panels doubles.

Taking these factors into account, smartest way to estimate systems payback time and economic feasibility is to have changing parameter on electricity cost, systems total investment and azimuth angle of the panels. Payback time represents the duration required for the system to recoup its initial investment. It is calculated by dividing the initial cost by the annual profits generated by the system.

$$T_{Payback} = \frac{C_{total\ investment}}{C_{Yearly\ savings} - C_{Yearly\ expanses}}$$

The yearly sales are calculated by dividing the hourly production E (W) by 1000, then multiplying it by sum the of various components: the variable electricity price (parameter z), electricity tax (0.063 cents/kWh), transfer tax (0.481 cents/kWh), and self-generated electricity tax (-0.261 cents/kWh). This resulting value is subsequently divided by 100 to convert into euros.

$$\text{Sales (€)} = \frac{\frac{E}{1000} \cdot (z + 0.063 + 0.481 - 0.261)\ \frac{cents}{kWh}}{100}$$

The yearly profits are determined by adding up the total sales for the year and deducting the corresponding expenses. The economic viability of the project can also be evaluated using metrics such as levelized cost of energy (LCOE), and net present value (NPV). Additionally, the project's reputation gain should be considered as another aspect of its feasibility. LCOE quantifies the cost of solar power production over a specified period, typically the warranted lifespan of the system. NPV assesses the profitability of the system by calculating the net present value of its future cash flows, considering factors such as the discount rate and operational years.

The LCOE is affected by the factors related to the production of the system such as the system losses, panel efficiency, orientation, and slope. The LCOE is calculated by dividing the total life cycle cost of the system by the total electricity produced over the life of the system. This takes into account the initial cost (I_0), the annual maintenance cost (M_T), the energy produced (E) and the degradation rate (y).

$$LCOE = \frac{Total\ lifetime\ costs}{Total\ lifetime\ output} = \frac{I_0 + \sum_{t=1}^{n} M_T}{\sum_{t=1}^{n} \frac{E}{(1+y)^t}}$$

The net present value of a project is calculated by calculating the net present value of the system for each year, adding them together and subtracting the initial investment. To calculate the annual NPV, the annual cash flows are divided by the discount factor. This coefficient is determined by adding one to the discount rate (r) and multiplying it by the power of the year of operation (t).

$$NPV = -Initial\ investment + \sum_{t=0}^{n} \frac{Cash\ flow}{(1+r)^t}$$

The payback time, LCOE and NPV will be calculate for two different panel systems with different slopes. The chosen slope angles are 20 and 30 degrees and aim to maximize the overall output given the limited roof space. Graphs 5 and 6 show payback times for different system combinations with 20 and 30 degree slope angles.

The calculations are based on panels with dimensions of 2 m x 1 m, a power output of 350 W and an efficiency of 18%. Considering the common yearly degradation rate of 0.5% for modern solar panels, yearly expenses amount to 2% of the system price, with system losses estimated at 30%, derived from current PV systems. The price of PV system is around 1100 €/kWp but the costs are experiencing a slight downward trend, prompting the selection of three system prices for this study: 1100 €/kWp, 1000 €/kWp and 900 €/kWp. Azimuth angles for these panels are chosen as -45°, 0° and 90°. It's noted from Table 1 that the differences between positive and negative angles of the same azimuth angle are negligible. This approach allows for the analysis of multiple angles simultaneously.

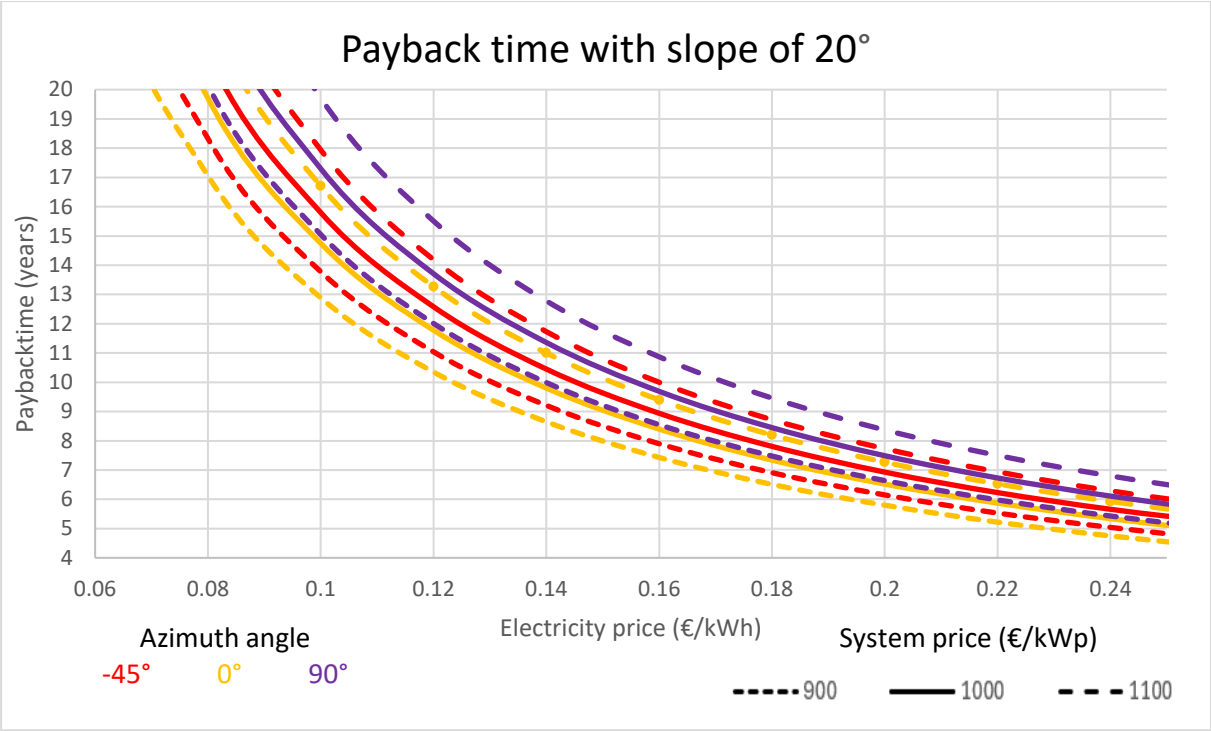

Graph 5. Payback time of solar panels with different azimuth angles and electricity prices at slope 20°.

Graph 5 illustrates that with an electricity price of 10 cents/kWh, the systems would achieve a minimum payback time of 12.5 years. Conversely, all the different systems would exhibit payback times under 20 years if the electricity price exceeds 18 cents/kWh.

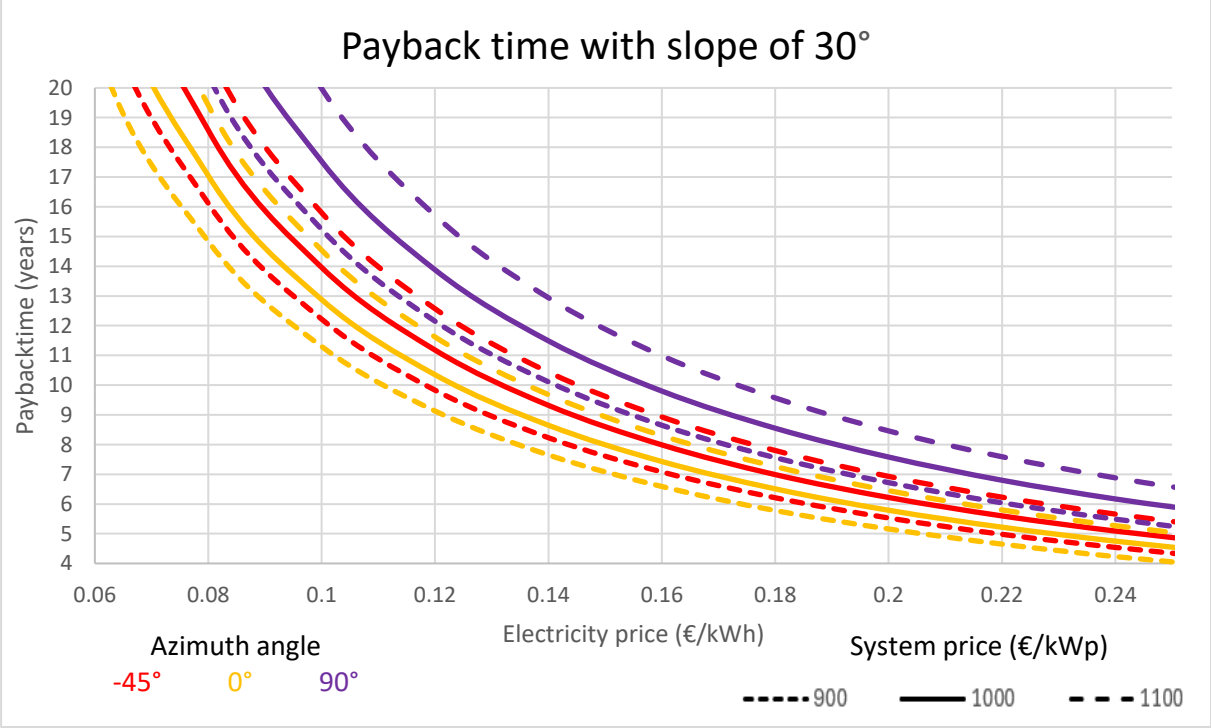

Graph 6. Payback times of solar panels with different azimuth angles and electricity prices at slope 30°.

Graph 6 illustrates that with an electricity price of 10 cents/kWh, the systems would achieve a minimum payback time of 11 years. Conversely, all the different systems would exhibit payback times under 10 years if the electricity price exceeds 18 cents/kWh. As shown in graphs 5 and 6, the payback times of these systems are dominantly dependent on the system price rather than the panel orientation or slope. However, it's noteworthy that systems with a 30-degree slope tend to exhibit shorter payback times. The LCOE values from table 2 reflect these findings accordingly. The LCOE values of the different systems are mainly below 10 cents/kWh, indicating that the electricity produced by the systems would cost less than 10 cents/kWh.

Table 2. LCOE of silicon solar panels with different slope and azimuth angles and different system prices.

LCOE (€/kWh)	Slope					
	20°			30°		
azimuth angle / system price (€/kWp)	-45°	0°	90°	-45°	0°	90°
900	0.07	0.07	0.08	0.07	0.06	0.08
1000	0.08	0.08	0.09	0.07	0.07	0.09
1100	0.09	0.08	0.09	0.08	0.08	0.10

The NPV calculations are done with the same parameters and dimension as those used for calculating the payback time. Two discount rates are considered: 3% and 8%. The 3% discount rate reflects a scenario similar to investment in a bank, while the 8% rate reflects investment in alternative means.

Table 3. Electricity prices, where solar panel system keeps its face value after 25 years of operation.

Electricity price (€/kWh) where PV system has kept its face value	Slope 20°						Slope 30°					
	r = 3%			r = 8%			r = 3%			r = 8%		
azimuth angle / system price (€/kWp)	-45°	0°	90°	-45°	0°	90°	-45°	0°	90°	-45°	0°	90°
900	0.16	0.15	0.17	0.24	0.23	0.26	0.14	0.13	0.17	0.22	0.21	0.26
1000	0.18	0.16	0.19	0.27	0.26	0.29	0.16	0.15	0.19	0.24	0.23	0.29
1100	0.19	0.18	0.21	0.3	0.28	0.32	0.18	0.17	0.21	0.27	0.25	0.32

NPV values offer a different perspective compared to payback periods and LCOE values, as they assess the profitability of the system and its potential increase in value over time. The table 3 describes what the electricity price needs to be in order that the system would keep its nominal

value after its lifetime. With a discount factor of 3%, the nominal value of the system is achieved with electricity price of 16-20 cents/kWh, which varies according to different system prices and azimuths. With a discount factor of 8 %, the range increases to 22-32 cents/kWh. This means that in 25 years the value of the system would be the same as today if the electricity price were as described above. If the electricity price falls, the system will not reach its nominal value, whereas if the price rises, the system will prove to be profitable.

At present, silicon solar panels are at the edge of the profitability of renewable energy production, given the current system and electricity prices and their yields. The low irradiation with low electricity prices brings a challenge to profitability. Meyer has more than 20 000 square metres of roof area, but only a fraction of this area - only a few thousand square metres - has a roof that is strong enough to support the weight of the solar system [148]. This means that a significant proportion of buildings and halls would require major renovation work to accommodate such solar energy systems.

CIGS thin-film panels could be an alternative for solar energy production on roofs where the weight of silicon solar panel systems is not suitable. However, it is important to note that the price of these CIGS thin-film panels is significantly higher than that of silicon solar panels. The cost of a CIGS thin-film panel system is generally three to four times higher than that of a silicon solar panel system.

On these roofs, with a pitch of about 5 degrees and an azimuth angle of 0-45 degrees, the difference in solar radiation efficiency between these azimuth angles is minimal, about 20 kWh/m^2. Therefore, the choice of azimuth angle doesn't have a significant impact on energy production, especially on roofs with such a low pitch. The example CIGS panels have dimension of 3 m x 0.5 m, power output of 250 W and efficiency of 17%. The payback period for these panels exceeds 70 years at an electricity price of 10 cents/kWh and a system price of 3 000 €/kWp. Even with a higher electricity price of 20 cents/kWh, the payback period would still be beyond 20 years. In Finland, the feasibility of these systems depends on the availability of substantial financial support to help mitigate high investment costs. Without such support, the large-scale deployment of CIGS panels would be economically impossible under current market conditions.

5.3.1.1 Noteworthy

The high loss percentage of the current panel system could be affected by dust accumulation on the panel. Dust accumulation in solar panels is a crucial factor that can significantly affect their efficiency and thus affect the accuracy of our calculations. In Finland, it usually rains regularly, which helps to clean the panels, but in areas such as shipyards, dust is constantly present due to the traffic. Without regular cleaning, dust accumulation can significantly reduce the output of solar panels. It is therefore essential to take this factor into account when assessing the feasibility and performance of solar panel installations, especially in environments such as shipyards where dust levels are high.

Also, it's worth remembering that these calculations are only estimates for different prices and scenarios and may not necessarily be accurate in every scenario. In reality, the prices of systems and panels may change in different ways than Swanson's law predicts.

5.3.2 Windpower

The wind data used in the calculations are from the Finnish Meteorological Institute [159]. Two different measurement sites have been used: Artukainen and Rajakari. Artukainen, located on the mainland about 3 km from Meyer, and Rajakari, located on an islet about 8 km from Meyer. The weather stations measure wind speeds every hour throughout the year. Although neither location fully reflects the conditions at Meyer and Meyer does not have wind data, the wind data from Artukainen and the average of both locations are used in the calculations. This causes a margin of error in these calculations, but these calculations are indicative. This approach is also based on the assumption that Meyer's actual wind speed is somewhere close to the average of these measurements. The wind data from Artukainen have yearly average of 2.89 m/s while data from Rajakari have average of 5.63 m/s.

The power output P (W) of a wind turbine can be calculated by:

$$P = \frac{1}{2} \cdot C_P \cdot \rho \cdot \eta \cdot A \cdot v^3$$

, where Cp is the power coefficient, ρ is the density of air ($\frac{kg}{m^3}$), A is the rotor swept area (m^2) and v is the wind speed ($\frac{m}{s}$). The power coefficient, known also as efficiency, has a theoretical maximum value of $\frac{16}{27}$ studied by Albert Betz [160]. The density of the air is dependent on the temperature of the air and therefore it also needs to be calculated. It can be calculated by:

$$\rho = \frac{p \cdot M}{R \cdot T}$$

, where p is the air pressure (kPa), M is the molecular mass of the air ($\frac{g}{mol}$), R is the gas constant ($\frac{J}{mol \cdot K}$), and T is the air temperature (K). The wind speed at different height can be calculated by:

$$W_1 = W_0 \cdot (\frac{z_1}{z_0})^a$$

, where W_1 represent the wind speed at the desired heigh, W_0 represent the wind speed at measured height, z_1 is the desired height, z_0 indicates the height of the measured location and a is the wind shear coefficient, which is generally considered to be $\frac{1}{7}$. The wind power output can also be determined by utilizing the power curve of the wind turbine. This involves categorizing the entire year's wind data based on wind speed and calculating the proportion for each category. Subsequently, the proportion is multiplied by the corresponding power output for each category, and these values are summed up to obtain the total output. However, for this thesis, the output will be calculated directly from equations rather than using this method.

As well as for the solar power system, various factors must be taken into account during the design of wind turbines. These include electricity and wind turbine system prices, which are often influenced by factors such as system power, efficiency, and wind speeds. As discussed in previous chapters, forecasting future electricity prices is challenging due to anticipated significant increases in production. Furthermore, wind power already plays a significant role in Finland's energy production, meaning that fluctuations in wind speeds have a substantial impact on Day-ahead prices. The price of a utility-scale horizontal wind turbine is close to 1€/1W and the price increases as the wind turbine sizes decreases [161]. The medium-scale horizontal wind turbine prices range from 1.75€/W to 3 €/W and the exact price depends on the manufacturer, efficiency, and size. Currently, efficiencies for medium-scale horizontal turbines are approximately around 40 %.

Given these considerations, the most effective approach to estimating the payback time and economic feasibility of wind turbine systems is to have changing parameters on electricity cost, wind speed as well as the system size and price. Similar economic assessment metrics used for PV systems, LCOE and NPV, will be applied. The estimation will focus on medium-scale HAWTs and small to medium-scale VAWTs. The utility-scale wind turbines are not suitable

for the site due to space constraints. By analysing these factors comprehensively, we can determine the viability of wind turbine systems for the given location.

Four different sizes of HAWTs are assessed: 20 kW, 30 kW, 50 kW, and 100 kW. The turbines have same the efficiencies but different sizes of rotors and masts. The 20 kW and 30 kW turbines have the same price category of 2-3 €/W, the 50 kW have a price category of 1.75-2.5 €/W and the 100 kW have price category of 1-2 €/W.

Table 4. Specifications of the turbines.

	Rotor blade (m)	Mast height (m)	Efficiency (%)
20 kW	5	20	40
30 kW	7.8	30	40
50 kW	8.6	30	40
100 kW	12.5	40	40

The yearly sales calculations are done the same way as for PV system. The yearly sales are calculated by dividing the hourly production E (W) by 1000, then multiplying it by sum of various components: the variable electricity price (parameter z), electricity tax (0.063 cents/kWh), transfer tax (0.616 cents/kWh) and self-generated electricity tax (-0.332 cents/kWh). This resulting value is subsequently divided by 100 to convert into euros.

$$\text{Sales (€)} = \frac{\frac{E}{1000} \cdot (z + 0.063 + 0.616 - 0.332)\,\frac{cents}{kWh}}{100}$$

The yearly profits are calculated by summing the yearly sales up and reducing the yearly expanses of it. The payback time, LCOE and NPV are calculated the same way as with PV systems.

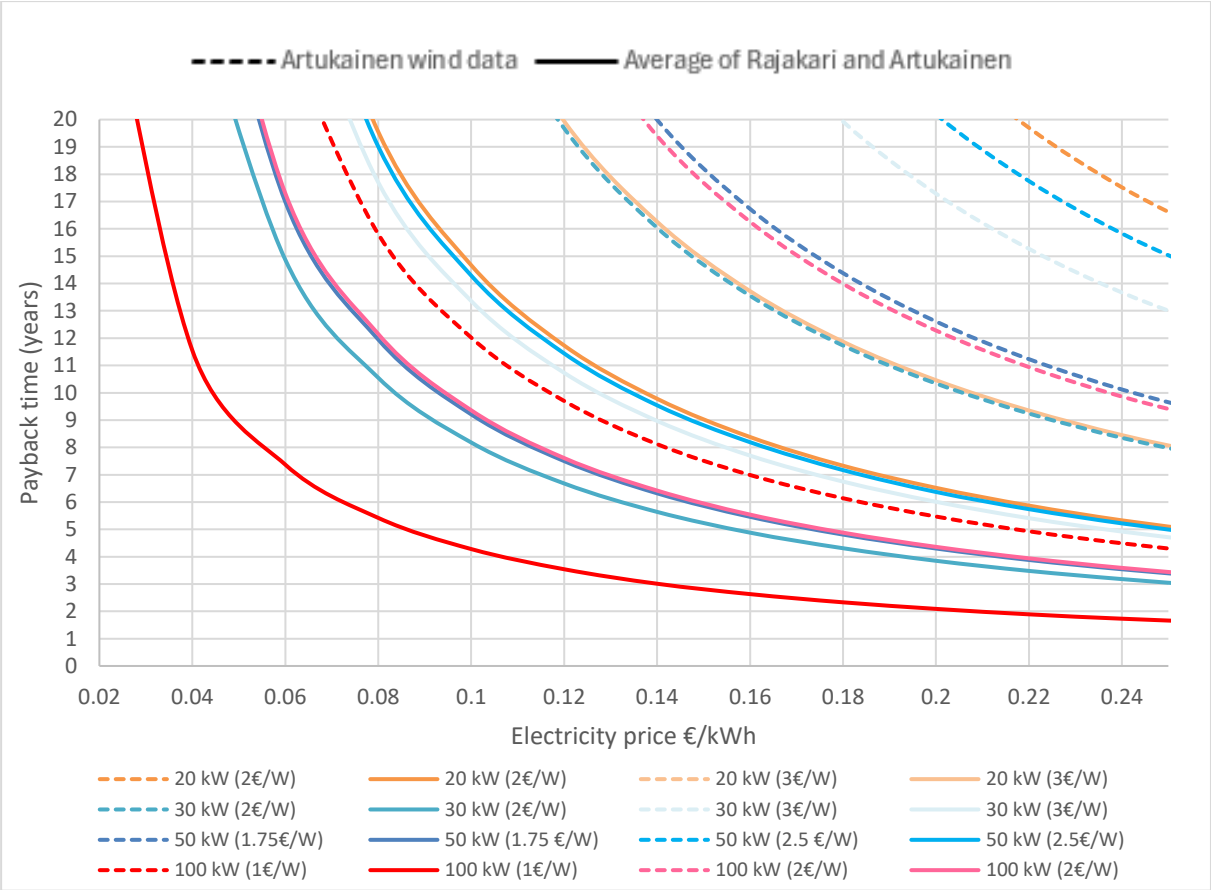

Graph 7. Payback times of different size wind turbines with different wind speeds and different electricity prices.

The payback times varies considerably between the different systems. Larger wind turbines tend to be more profitable than smaller ones, mainly because wind speeds are steadier and higher at greater altitudes. Moreover, energy production increases significantly due to the cubic relationship between wind speed and power output. Additionally, larger wind turbines often have a lower cost per unit of energy produced compared to smaller ones, further contributing to their profitability.

Both the LCOE values and payback times highlight the significant influence of wind speeds and system sizes on the results. LCOE values calculated using wind speeds from Artukainen suggest that most systems are not economically feasible. However, when incorporating the average wind speeds from Artukainen and Rajakari, nearly all systems become financially viable. This highlights the critical importance of accurate wind speed data and careful consideration of system sizes in assessing the economic viability of wind turbine installations.

Table 5. LCOE of HAWT with different turbine sizes, prices, and wind speeds.

LCOE (€/kWh)	Turbine size							
	20 kW		30 kW		50 kW		100 kW	
Price of the system (€/W) / Wind speed location	2	3	2	3	1.75	2.5	1	2
Artukainen	0.21	0.31	0.11	0.17	0.13	0.19	0.07	0.13
Average of Artukainen and Rajakari	0.08	0.12	0.05	0.07	0.05	0.08	0.03	0.05

The NPV calculations are done solely using average wind data, primarily as the Artukainen wind speeds indicate that most systems are not economically feasible.

Table 6. Electricity price (€), where wind turbine system keeps its face value after 30 years of operation.

Electricity price (€/kWh) where WT system has kept its face value	Turbine size							
	20 kW		30 kW		50 kW		100 kW	
Price of the system (€/W) / Discount factor	2	3	2	3	1.75	2.5	1	2
3%	0.15	0.22	0.10	0.13	0.10	0.14	0.05	0.10
8%	0.24	0.34	0.15	0.22	0.16	0.24	0.08	0.16

Table 6 shows the electricity price which corresponds to the point where the system reaches its nominal value. Below this limit, the system becomes economically profitable. From an investor's point of view, investing in a 100 kW turbine at a system price of 1 €/W is considered a most profitable investment. For example, at an electricity price of 10 cents/kWh, the value of the system increases by 248% and 61% with discount rates of 3% and 8% respectively. With a discount factor of 8%, the other systems would not be economically viable, while with a discount factor of 3%, half of the systems would maintain their nominal value after 30 years if the electricity price remained at 10 cents/kWh. As prices fall, systems become economically viable, while as they rise, the systems don't maintain their nominal value.

The analysis of the economic feasibility of VAWT provides a straightforward result as it won't be a viable option for production at this time. At current prices of 3-7.5 €/W and efficiencies of 30%, the payback period and LCOE of VAWTs are extremely high, making them an unviable option. The prices and efficiencies of VAWTs would have to be significantly improved to make

them a viable option for electricity generation in this location. At present, it is more cost-effective to rely on the grid than to generate electricity independently with VAWTs.

Table 7. LCOE of VAWT on different turbine sizes, system prices and wind speeds.

LCOE (€/kWh)	Turbine size					
	5kW			7.5kW		
Price of the system (k€/kW) / Wind speed location	3	5	7.5	3	5	7.5
Artukainen	0.37	0.62	0.93	0.64	1.07	1.61
Average of Artukainen and Rajakari	0.14	0.23	0.35	0.23	0.38	0.58

From table 7 can be seen the different LCOE values with different system combinations. Even with the smallest LCOE value of 0.14 €/kWh, achieved with a 5kW turbine, system price of 3 €/W, and wind speed from the average of the measuring points at Artukainen and Rajakari, VAWTs remain an unviable option.

While emerging wind power systems show promise, they are still in the development phase, making their efficiencies and feasibility uncertain. However, companies like Kitemill estimate that their airborne wind turbine solution could potentially produce energy at costs below 0.10 €/kWh. Nonetheless, this remains an estimation, and further research and development are needed to determine the true viability of these innovative systems.

5.3.2.1 Wind turbine location

It can be said that the larger wind turbines that were examined are feasible, but the main problem is the site and its location. Turbines need hundreds of metres of safety clearance to the nearest obstacles. The necessary space is first needed to find and then comes second problem which is the location. The coastal fleets base locates in the nearby as well as residential apartments. There has been put a law by the Finnish Government which has defined limit values for the noise from wind turbines. These limits are 45 dB for the housing in the daytime and in nighttime 40 dB [162]. According to the wind association noise from utility-scale wind turbines is lower that these limits from distance of 700-1000 metres [163]. This means that the turbines could be built if suitable space is available and the space in question is to be used for renewable energy production and not for the expansion of the shipyard. This requires further investigation in any case and is one of the next things to be done alongside the wind speed measurements at Meyer's Turku site.

5.3.2.2 Noteworthy

It's crucial to understand that these calculations serve as a tool for considering the profitability of wind power in the specific location. The wind speed measurements may not be entirely accurate as it was not possible to acquire the exact wind data. The variability in wind turbine system prices is combination from multiple manufacturers. If the decision to invest in wind power is made and detailed planning initiated, it will necessitate to make also new and more comprehensive calculations. These calculations should include the exact wind speed at the actual location and then compare it with the pricing and stated output of the selected manufacturer's turbine.

5.3.3 Energy aid

Business Finland is aiding projects that promote new technology, its commercial utilization, and the regulation capacity of the power system, as well as energy savings through energy efficiency [164]. However, there are no specific guidelines regarding what constitutes a new technology. While solar and wind power have been on the market for over a decade, they may still be considered new in terms of ongoing advancements and innovations, especially with regards to emerging technologies such as thin film solar panels. Similarly, VAWTs have been around since the 1950s, but their utilization has historically been lower compared to HAWTs. Thus, VAWTs could still be considered a new or emerging technology, particularly if there are ongoing developments or increased adoption rates. While projects involving new technology may be eligible for support from Business Finland, it's important not to overly rely on this aid in calculations. Instead, it should be considered as a potential factor but not the sole determinant of feasibility.

5.4 Energy storage, energy independence and sustainability

In terms of renewable energy storage, its benefits are currently limited. In the absence of a clear solution for efficient energy storage, the potential benefits of storage are negligible, given the current limited electricity production. However, when production volumes reach the current base load, it becomes recommended to explore the feasibility and profitability of energy storage investments. It is likely that this will not become a pressing issue for some time, and as the plans advance, there will be opportunities to conduct these feasibility studies. The benefits of the energy storage at that time are hard to forecast and it’s anticipated that energy storage solutions will continue to evolve, necessitating a more comprehensive study in the future.

Achieving full energy independency at Meyer Turku is not possible at present or near future. However, efforts can be made to increase the share of self-generated electricity. Currently, this number stands at around 0.5%, and there is a lot of room for improvement. Therefore, the focus should not be only increasing the energy production but also reducing overall energy consumption.

It should be noted that increasing the shipyard's own renewable energy sources will not affect Meyer Turku's greenhouse gas emissions, as Meyer Turku is committed to its future promises and has only used certified carbon neutral electricity since 2018. In addition, from 2023 onwards, all district heating used at the shipyard have also been carbon neutral.

6 Conclusion

The purpose of this thesis was to create a comprehensive literature review on renewable energy and energy storage systems. The purpose was also to clarify the current energy management within the shipyard as well as estimate the feasibility of implementing renewable energy systems at the shipyard.

The amount of renewable energy is increasing and the ways to produce it are more diverse than ever. New production systems are being explored and developed, as are ways of storing harnessed energy. However, the low price of electricity in Finland poses a challenge to the adoption of renewable energy in business. In this thesis, different solar and wind power systems were analysed under different scenarios, where electricity price, system price, system size and system location were variables.

Solar energy systems with different azimuth and slope angles alongside different system prices produced LCOE values of 0.10 €/kWh or less. Payback times varied significantly, with the configuration of a slope of 30 degrees, azimuth of 0 degrees, and system price of 900 €/kWp achieving a payback time of 11 years at an electricity cost of 10 cents/kWh. The CIGS thin films panels proved to be too expensive to invest without substantial subsidies. As anticipated the HAWTs outperformed the VAWTs with HAWTs producing LCOE values ranging from 0.03 €/kWh to 0.21 €/kWh, whereas VAWTs produced LCOE values over 0.21 €/kWh, with some exceeding 1€/kWh. Notably, four different-sized turbines achieved payback times under 10 years at an electricity cost of 10 cents/kWh, with the most profitable configuration being 100 kW turbine with a system price of 1€/W and average wind speed from Artukainen and Rajakari. In PV systems, the system price had the largest impact, while in wind power, turbine size and wind speed had the largest impact.

In summary, it is possible to use renewable energy sources in a shipyard, as long as a suitable location is found. Although the implementation of a large-scale solar energy system is currently impractical due to the poor condition of the buildings and roofs, it could be considered in the context of future renovation projects. Alternatively, the integration of wind turbines is a viable investment option, although it requires further studies to determine the exact location and wind speed. Overall, both solar and wind energy offer promising opportunities to reduce dependence on conventional energy sources in the yard.

Renewable energy sources are paving the way for a greener tomorrow and integrating them into the maritime sector could prove to be a valuable asset in an evolving world. In this transition, companies need to consider their desired payback period and the value placed on the social aspect of sustainability.

The essential point is how much companies are willing to invest in sustainability and the importance they attach to the social dimension, including the image of a greener company. By prioritising sustainability initiatives and adopting renewable energy solutions, companies could reduce their environmental footprint and improve their reputation while also appealing to those who value corporate social responsibility. Ultimately, the decision to invest in renewables reflects a commitment to both environmental protection and long-term business success in an increasingly environmentally aware world.

In the context of this work, the next step is to find out why the system losses of existing solar panels are so high. On a more general level, questions related to Meyer Turku's consumption should be addressed, such as why the current base load is so high and where exactly it is consumed? How this could be reduced and how the energy efficiency of the yard could be improved? As regards energy efficiency, it would be particularly useful to investigate waste heat recovery and heat storage.

References

[1] NEcOLEAP, “Ecosystem,” 2024. https://necoleap.fi/.

[2] World Energy Council, “Energy resources: Solar,” *World Energy Counc. 2013 World Energy Resour. Sol.*, p. 28, 2013.

[3] EU, “Photovoltaic geographical information system (PVGIS),” 2022. https://re.jrc.ec.europa.eu/pvg_tools/en/.

[4] G. Dr. Kopp, “Total solar irradiance data,” *Laboratory for Atmospheric and Space Physics*, 2024. https://lasp.colorado.edu/sorce/data/tsi-data/.

[5] R. Seppänen *et al.*, *MAOL taulukot*, 1.-3. Kustannusosakeyhtiö Otava, 2014.

[6] K. E. Trenberth, J. T. Fasullo, and J. Kiehl, “Earth’s global energy budget,” *Bull. Am. Meteorol. Soc.*, vol. 90, no. 3, 2009, doi: 10.1175/2008BAMS2634.1.

[7] H. Ritchie, P. Rosaldo, and M. Roser, “Energy production and consumption,” *OurWorldInData.org.*, 2020. https://ourworldindata.org/energy-production-consumption.

[8] P. Bojek, “Solar pv,” *iea.org*, 2024. https://www.iea.org/energy-system/renewables/solar-pv.

[9] Landartgenerator, “Total surface area required to fuel the world with solar,” *landartgenerator.org*, 2009. https://landartgenerator.org/blagi/archives/127.

[10] D. Barlev, R. Vidu, and P. Stroeve, “Innovation in concentrated solar power,” *Solar Energy Materials and Solar Cells*, vol. 95, no. 10. 2011, doi: 10.1016/j.solmat.2011.05.020.

[11] S. A. Kalogirou, “Solar thermal collectors and applications,” *Progress in Energy and Combustion Science*, vol. 30, no. 3. 2004, doi: 10.1016/j.pecs.2004.02.001.

[12] D. Krüger, S. Fischer, T. Hirsch, and J. I. Labairu, “Concentrating solar systems in moderate climates,” in *AIP Conference Proceedings*, 2022, vol. 2445, doi: 10.1063/5.0085792.

[13] B. Perers, S. Furbo, and J. Dragsted, “Thermal performance of concentrating tracking solar collectors,” 2013.

[14] Motiva, “Auringonsäteilyn määrä Suomessa,” 2024. https://www.motiva.fi/ratkaisut/uusiutuva_energia/aurinkosahko/aurinkosahkon_perusteet/auringonsateilyn_maara_suomessa.

[15] A. Goetzberger, J. Knobloch, B. Vos, and R. Waddington, *Crystalline silicon solar cells*. wiley, 2014.

[16] P. Kar, *Doping in conjugated polymers*, 1st ed. Hoboken, New Jersey: John Wiley and Sons, Inc., 2013.

[17] N. Y. Di Carlo, Aldo; Lamanna, Enrico; Nia, "Photovoltaics," *EPJ Web Conf.*, vol. 246, pp. 171–202, 2020, doi: 10.1051/epjconf/202024600005.

[18] TU DELFT, "Performance and optimization," *owc.tudelf.nl*, 2024. https://ocw.tudelft.nl/course-lectures/solar-cells-l4-perf-optimization/.

[19] W. Shockley and H. J. Queisser, "Detailed balance limit of efficiency of p-n junction solar cells," *J. Appl. Phys.*, vol. 32, no. 3, 1961, doi: 10.1063/1.1736034.

[20] J. F. Guillemoles, T. Kirchartz, D. Cahen, and U. Rau, "Guide for the perplexed to the Shockley–Queisser model for solar cells," *Nature Photonics*, vol. 13, no. 8. 2019, doi: 10.1038/s41566-019-0479-2.

[21] C. H. Henry, "Limiting efficiencies of ideal single and multiple energy gap terrestrial solar cells," *J. Appl. Phys.*, vol. 51, no. 8, 1980, doi: 10.1063/1.328272.

[22] T. Tiedje, E. Yablonovitch, G. D. Cody, and B. G. Brooks, "Limiting efficiency of silicon solar cells," *IEEE Trans. Electron Devices*, vol. 31, no. 5, 1984, doi: 10.1109/T-ED.1984.21594.

[23] T. D. Lee and A. U. Ebong, "A review of thin film solar cell technologies and challenges," *Renewable and Sustainable Energy Reviews*, vol. 70. 2017, doi: 10.1016/j.rser.2016.12.028.

[24] D. Soler, M. Fonrodona, C. Voz, J. M. Asensi, J. Bertomeu, and J. Andreu, "Substrate influence on the properties of doped thin silicon layers grown by Cat-CVD," in *Thin Solid Films*, 2003, vol. 430, no. 1–2, doi: 10.1016/S0040-6090(03)00095-6.

[25] K. L. Chopra, P. D. Paulson, and V. Dutta, "Thin-film solar cells: An overview," *Prog. Photovoltaics Res. Appl.*, vol. 12, no. 2–3, 2004, doi: 10.1002/pip.541.

[26] S. Ray, R. Das, and A. K. Barua, "Performance of double junction a-Si solar cells by using ZnO:Al films with different electrical and optical properties at the n/metal interface," *Sol. Energy Mater. Sol. Cells*, vol. 74, no. 1–4, 2002, doi: 10.1016/S0927-0248(02)00128-9.

[27] M. M. Aliyu *et al.*, "Recent developments of flexible CdTe solar cells on metallic substrates: Issues and prospects," *International Journal of Photoenergy*, vol. 2012. 2012, doi: 10.1155/2012/351381.

[28] R. Sharma, Himanshu, S. L. Patel, S. Chander, M. D. Kannan, and M. S. Dhaka, "Physical properties of ZnSe thin films: Air and vacuum annealing evolution to buffer layer applications," *Phys. Lett. Sect. A Gen. At. Solid State Phys.*, vol. 384, no. 4, 2020,

doi: 10.1016/j.physleta.2019.126097.

[29] G. Kartopu *et al.*, “Enhancement of the photocurrent and efficiency of CdTe solar cells suppressing the front contact reflection using a highly-resistive ZnO buffer layer,” *Sol. Energy Mater. Sol. Cells*, vol. 191, 2019, doi: 10.1016/j.solmat.2018.11.002.

[30] M. K. S. Bin Rafiq *et al.*, “WS2: A New window layer material for solar cell application,” *Sci. Rep.*, vol. 10, no. 1, 2020, doi: 10.1038/s41598-020-57596-5.

[31] R. S. Hall, D. Lamb, and S. J. C. Irvine, “Back contacts materials used in thin film CdTe solar cells—A review,” *Energy Science and Engineering*, vol. 9, no. 5. 2021, doi: 10.1002/ese3.843.

[32] V. Narayanan and R. Ks, “CdTe photovoltaics in superstrate geometry-back-contact materials: A review,” *ACS Applied Energy Materials*, vol. 6, no. 17. 2023, doi: 10.1021/acsaem.3c00947.

[33] A. S. Mohamed and H. A. Mohamed, “Modelling of high-efficiency substrate CIGS solar cells with ultra-thin absorber layer,” *Indian J. Phys.*, vol. 94, no. 11, 2020, doi: 10.1007/s12648-019-01626-0.

[34] W. Li, X. Yan, W. L. Xu, J. Long, A. G. Aberle, and S. Venkataraj, “Efficiency improvement of CIGS solar cells by a modified rear contact,” *Sol. Energy*, vol. 157, 2017, doi: 10.1016/j.solener.2017.08.054.

[35] M. Younas, T. A. Kandiel, A. Rinaldi, Q. Peng, and A. A. Al-Saadi, “Ambient-environment processed perovskite solar cells: A review,” *Mater. Today Phys.*, vol. 21, no. October, 2021, doi: 10.1016/j.mtphys.2021.100557.

[36] N. Suresh Kumar and K. Chandra Babu Naidu, “A review on perovskite solar cells (PSCs), materials and applications,” *J. Mater.*, vol. 7, no. 5, 2021, doi: 10.1016/j.jmat.2021.04.002.

[37] T. Lemercier, L. Perrin, E. Planès, S. Berson, and L. Flandin, “A comparison of the structure and properties of opaque and semi-transparent NIP/PIN-type scalable perovskite solar cells,” *Energies*, vol. 13, no. 15, 2020, doi: 10.3390/en13153794.

[38] A. Kojima, K. Teshima, Y. Shirai, and T. Miyasaka, “Organometal halide perovskites as visible-light sensitizers for photovoltaic cells,” *J. Am. Chem. Soc.*, vol. 131, no. 17, 2009, doi: 10.1021/ja809598r.

[39] J. Y. Jeng *et al.*, “CH3NH3PbI3 perovskite/fullerene planar-heterojunction hybrid solar cells,” *Adv. Mater.*, vol. 25, no. 27, 2013, doi: 10.1002/adma.201301327.

[40] M. Green, E. Dunlop, J. Hohl-Ebinger, M. Yoshita, N. Kopidakis, and X. Hao, “Solar cell efficiency tables (version 57),” *Prog. Photovoltaics Res. Appl.*, vol. 29, no. 1,

2021, doi: 10.1002/pip.3371.

[41] T. Ji *et al.*, “Charge transporting materials for perovskite solar cells,” *Rare Metals*, vol. 40, no. 10. 2021, doi: 10.1007/s12598-021-01723-2.

[42] X. Zhao and M. Wang, “Organic hole-transporting materials for efficient perovskite solar cells,” *Materials Today Energy*, vol. 7. 2018, doi: 10.1016/j.mtener.2017.09.011.

[43] L. Qiu, L. K. Ono, and Y. Qi, “Advances and challenges to the commercialization of organic–inorganic halide perovskite solar cell technology,” *Materials Today Energy*, vol. 7. pp. 169–189, 2018, doi: 10.1016/j.mtener.2017.09.008.

[44] S. Jouttijärvi *et al.*, “A comprehensive methodological workflow to maximize solar energy in low-voltage grids: A case study of vertical bifacial panels in Nordic conditions,” *Sol. Energy*, vol. 262, 2023, doi: 10.1016/j.solener.2023.111819.

[45] R. Guerrero-Lemus, R. Vega, T. Kim, A. Kimm, and L. E. Shephard, “Bifacial solar photovoltaics - A technology review,” *Renewable and Sustainable Energy Reviews*, vol. 60. 2016, doi: 10.1016/j.rser.2016.03.041.

[46] Z. Fang *et al.*, “Perovskite-based tandem solar cells,” *Science Bulletin*, vol. 66, no. 6. 2021, doi: 10.1016/j.scib.2020.11.006.

[47] T. Leijtens, K. A. Bush, R. Prasanna, and M. D. McGehee, “Opportunities and challenges for tandem solar cells using metal halide perovskite semiconductors,” *Nature Energy*, vol. 3, no. 10. 2018, doi: 10.1038/s41560-018-0190-4.

[48] M. Heydarian *et al.*, “Monolithic two-terminal perovskite/perovskite/silicon triple-junction solar cells with open circuit voltage >2.8 V,” *ACS Energy Lett.*, vol. 8, no. 10, 2023, doi: 10.1021/acsenergylett.3c01391.

[49] H. Shen *et al.*, “Mechanically-stacked perovskite/CIGS tandem solar cells with efficiency of 23.9% and reduced oxygen sensitivity,” *Energy Environ. Sci.*, vol. 11, no. 2, pp. 394–406, 2018, doi: 10.1039/c7ee02627g.

[50] J. Liu, S. Lu, L. Zhu, X. Li, and W. C. H. Choy, “Perovskite-organic hybrid tandem solar cells using a nanostructured perovskite layer as the light window and a PFN/doped-MoO3/MoO3 multilayer as the interconnecting layer,” *Nanoscale*, vol. 8, no. 6, pp. 3638–3646, 2016, doi: 10.1039/c5nr07457f.

[51] K. Xiao *et al.*, “All-perovskite tandem solar cells with 24.2% certified efficiency and area over 1 cm2 using surface-anchoring zwitterionic antioxidant,” *Nat. Energy*, vol. 5, no. 11, 2020, doi: 10.1038/s41560-020-00705-5.

[52] B. Chen *et al.*, “Enhanced optical path and electron diffusion length enable high-efficiency perovskite tandems,” *Nat. Commun.*, vol. 11, no. 1, 2020, doi:

10.1038/s41467-020-15077-3.

[53] L. Meng *et al.*, “Organic and solution-processed tandem solar cells with 17.3% efficiency,” *Science (80-.).*, vol. 361, no. 6407, 2018, doi: 10.1126/science.aat2612.

[54] K. Kim *et al.*, “Simulations of chalcopyrite/c-Si tandem cells using SCAPS-1D,” *Sol. Energy*, vol. 145, 2017, doi: 10.1016/j.solener.2017.01.031.

[55] T. I. Alanazi and M. El Sabbagh, “Proposal and design of flexible all-polymer/CIGS tandem solar cell,” *Polymers (Basel).*, vol. 15, no. 8, 2023, doi: 10.3390/polym15081823.

[56] A. K. Patel, R. Mishra, S. K. Soni, P. K. Rao, and O. Mishra, “Design and performance investigation of CIGS/SWCNT tandem solar cell for efficiency improvement,” *Opt. Commun.*, vol. 559, no. December 2023, p. 130392, 2024, doi: 10.1016/j.optcom.2024.130392.

[57] S. et al. Liu, “Triple-junction solar cells with cyanate in ultrawide bandgap perovskites,” *Nature*, 2024, doi: 10.1038/s41586-024-07226-1.

[58] N. Martín-Chivelet *et al.*, “Building-integrated photovoltaic (BIPV) products and systems: A review of energy-related behavior,” *Energy Build.*, vol. 262, 2022, doi: 10.1016/j.enbuild.2022.111998.

[59] Department of Energy, “Solar roofing shingles,” 1998.

[60] AGC Active glass, “Energy-generating glass,” 2024. https://agc-activeglass.com/sunewat/.

[61] W. Li, C. Lin, G. Huang, J. Hur, B. Huang, and S. Yao, “Selective solar harvesting windows for full-spectrum utilization,” *Adv. Sci.*, vol. 9, no. 21, 2022, doi: 10.1002/advs.202201738.

[62] A. Ghosh, “Potential of building integrated and attached/applied photovoltaic (BIPV/BAPV) for adaptive less energy-hungry building’s skin: A comprehensive review,” *Journal of Cleaner Production*, vol. 276. 2020, doi: 10.1016/j.jclepro.2020.123343.

[63] A. Divya, T. Adish, P. Kaustubh, and P. S. Zade, “Review on recycling of solar modules/panels,” *Solar Energy Materials and Solar Cells*, vol. 253. 2023, doi: 10.1016/j.solmat.2022.112151.

[64] G. A. Heath *et al.*, “Research and development priorities for silicon photovoltaic module recycling to support a circular economy,” *Nat. Energy*, vol. 5, no. 7, 2020, doi: 10.1038/s41560-020-0645-2.

[65] M. Peplow, “Solar panels face recycling challenge,” *ACS Cent. Sci.*, vol. 8, no. 3, 2022,

doi: 10.1021/acscentsci.2c00214.

[66] R. Deng, Y. Zhuo, and Y. Shen, “Recent progress in silicon photovoltaic module recycling processes,” *Resources, Conservation and Recycling*, vol. 187. 2022, doi: 10.1016/j.resconrec.2022.106612.

[67] P. R. Dias *et al.*, “High yield, low cost, environmentally friendly process to recycle silicon solar panels: Technical, economic and environmental feasibility assessment,” *Renew. Sustain. Energy Rev.*, vol. 169, 2022, doi: 10.1016/j.rser.2022.112900.

[68] M. S. Chowdhury *et al.*, “An overview of solar photovoltaic panels’ end-of-life material recycling,” *Energy Strategy Reviews*, vol. 27. 2020, doi: 10.1016/j.esr.2019.100431.

[69] A. H.Kermani, “From rocks to solar cells: Silicon as the beating heart of solar panels,” *NTNU*, 2021. https://www.ntnu.no/blogger/teknat/2021/11/02/from-rocks-to-solar-cells-silicon-as-the-beating-heart-of-solar-panels/.

[70] I. D’Adamo, M. Miliacca, and P. Rosa, “Economic feasibility for recycling of waste crystalline silicon photovoltaic modules,” *Int. J. Photoenergy*, vol. 2017, 2017, doi: 10.1155/2017/4184676.

[71] R. Deng, N. L. Chang, Z. Ouyang, and C. M. Chong, “A techno-economic review of silicon photovoltaic module recycling,” *Renewable and Sustainable Energy Reviews*, vol. 109. 2019, doi: 10.1016/j.rser.2019.04.020.

[72] M. Tao *et al.*, “Major challenges and opportunities in silicon solar module recycling,” *Prog. Photovoltaics Res. Appl.*, vol. 28, no. 10, 2020, doi: 10.1002/pip.3316.

[73] K. Miettunen and A. Santasalo-Aarnio, “Eco-design for dye solar cells: From hazardous waste to profitable recovery,” *J. Clean. Prod.*, vol. 320, 2021, doi: 10.1016/j.jclepro.2021.128743.

[74] D. Polverini, N. Espinosa, U. Eynard, E. Leccisi, F. Ardente, and F. Mathieux, “Assessing the carbon footprint of photovoltaic modules through the EU Ecodesign Directive,” *Sol. Energy*, vol. 257, 2023, doi: 10.1016/j.solener.2023.04.001.

[75] NREL, “Life cycle greenhouse gas emissions from solar photovoltaics,” 2012.

[76] S. Gerbinet, S. Belboom, and A. Léonard, “Life cycle analysis (LCA) of photovoltaic panels: A review,” *Renewable and Sustainable Energy Reviews*, vol. 38. 2014, doi: 10.1016/j.rser.2014.07.043.

[77] Intergovernmental Panel on Climate Change, “Technology-specific cost and performance parameters,” in *Climate Change 2014: Mitigation of Climate Change*, 2015.

[78] A. Turgeon and E. Morse, “Wind,” 2023. https://education.nationalgeographic.org/resource/wind/.

[79] T. M. Letcher, *Wind energy engineering: A handbook for onshore and offshore wind turbines*, 2nd ed. London, England: Academic Press, 2023.

[80] M. et. al Wiatros-Motyka, “Global electricity review 2023,” 2023.

[81] M. Hutchinson and F. Zhao, “Global wind report 2023,” 2023.

[82] L.-F. Garcia-Rodriguez, J. Diego Rosero Ariza, J. Luis Chacón Velazco, and J. Ernesto Jaramillo Ibarra, “Vertical axis wind turbine design and installation at chicamocha canyon,” in *Entropy and Exergy in Renewable Energy*, 2022.

[83] G. Bedon, E. G. A. Antonini, S. De Betta, M. Raciti Castelli, and E. Benini, “Evaluation of the different aerodynamic databases for vertical axis wind turbine simulations,” *Renewable and Sustainable Energy Reviews*, vol. 40. 2014, doi: 10.1016/j.rser.2014.07.126.

[84] R. Kumar, K. Raahemifar, and A. S. Fung, “A critical review of vertical axis wind turbines for urban applications,” *Renewable and Sustainable Energy Reviews*, vol. 89. 2018, doi: 10.1016/j.rser.2018.03.033.

[85] N. Jenkins, T. Burton, E. Bossanyi, D. Sharpe, and M. Graham, *Wind energy handbook*, 3rd ed. John Wiley & Sons, 2021.

[86] A. Vasel-Be-Hagh and D. S. K. Ting, *Utility-scale wind turbines and wind farms*. Institution of Engineering & Technology, 2021.

[87] J. S. Savonius, “Rotor adapted to be driven by wind or flowing water,” US1697574A, 1929.

[88] J. S. Savonius, “Wind rotor,” US1766765A, 1930.

[89] D. Hilewit, E. A. Matida, A. Fereidooni, H. Abo el Ella, and F. Nitzsche, “Power coefficient measurements of a novel vertical axis wind turbine,” *Energy Sci. Eng.*, vol. 7, no. 6, 2019, doi: 10.1002/ese3.412.

[90] G. J. M. Darrieus, “Turbine having its rotating shaft transverse to the flow of the current,” US1835018A, 1931.

[91] B. Hand, G. Kelly, and A. Cashman, “Aerodynamic design and performance parameters of a lift-type vertical axis wind turbine: A comprehensive review,” *Renewable and Sustainable Energy Reviews*, vol. 139. 2021, doi: 10.1016/j.rser.2020.110699.

[92] E. Möllerström, P. Gipe, J. Beurskens, and F. Ottermo, “A historical review of vertical axis wind turbines rated 100 kW and above,” *Renewable and Sustainable Energy*

Reviews, vol. 105. 2019, doi: 10.1016/j.rser.2018.12.022.

[93] M. M. Aslam Bhutta, N. Hayat, A. U. Farooq, Z. Ali, S. R. Jamil, and Z. Hussain, "Vertical axis wind turbine: A review of various configurations and design techniques," *Renewable and Sustainable Energy Reviews*, vol. 16, no. 4. 2012, doi: 10.1016/j.rser.2011.12.004.

[94] K. K. Sharma, A. Biswas, and R. Gupta, "Performance measurement of a three-bladed combined Darrieus-Savonius rotor," *Int. J. Renew. Energy Res.*, vol. 3, no. 4, 2013.

[95] D. Bobrova, "Building-integrated wind turbines in the aspect of architectural shaping," in *Procedia Engineering*, 2015, vol. 117, no. 1, doi: 10.1016/j.proeng.2015.08.185.

[96] J. Park, H. J. Jung, S. W. Lee, and J. Park, "A new building-integrated wind turbine system utilizing the building," *Energies*, vol. 8, no. 10, 2015, doi: 10.3390/en81011846.

[97] J. Mortimer, "Why Elephant and Castle's iconic Strata tower wind turbines barely move," *MyLondon*, 2023. https://www.mylondon.news/news/south-london-news/elephant-castles-iconic-strata-tower-23551686.

[98] Eindhoven Univeristy of Technology, "Bahrain World Trade Center is exactly the wrong way round," 2014. https://www.tue.nl/en/news/news-overview/bahrain-world-trade-center-is-exactly-the-wrong-way-round.

[99] W. Baker, C. Besjak, B. McElhatten, and X. Li, "Pearl river tower: Design integration towards sustainability," 2014, doi: 10.1061/9780784413357.067.

[100] Windside, "Pearl River Tower in the City of the Immortals," 2018. https://windside.com/pearl-river-tower/.

[101] T. Sharpe and G. Proven, "Crossflex: Concept and early development of a true building integrated wind turbine," *Energy Build.*, vol. 42, no. 12, 2010, doi: 10.1016/j.enbuild.2010.07.032.

[102] H. K. Jani, S. Singh Kachhwaha, G. Nagababu, and A. Das, "A brief review on recycling and reuse of wind turbine blade materials," *Mater. Today Proc.*, vol. 62, no. P13, 2022, doi: 10.1016/j.matpr.2022.02.049.

[103] M. Y. Khalid, Z. U. Arif, M. Hossain, and R. Umer, "Recycling of wind turbine blades through modern recycling technologies: A road to zero waste," *Renewable Energy Focus* , vol. 44. 2023, doi: 10.1016/j.ref.2023.02.001.

[104] S. Karuppannan Gopalraj and T. Kärki, "A review on the recycling of waste carbon fibre/glass fibre-reinforced composites: Fibre recovery, properties and life-cycle analysis," *SN Applied Sciences*, vol. 2, no. 3. 2020, doi: 10.1007/s42452-020-2195-4.

[105] S. Sorte, N. Martins, M. S. A. Oliveira, G. L. Vela, and C. Relvas, “Unlocking the potential of wind turbine blade recycling: Assessing techniques and metrics for sustainability,” *Energies*, vol. 16, no. 22, 2023, doi: 10.3390/en16227624.

[106] A. Ahrens *et al.*, “Catalytic disconnection of C–O bonds in epoxy resins and composites,” *Nature*, vol. 617, no. 7962, 2023, doi: 10.1038/s41586-023-05944-6.

[107] M. Rani, P. Choudhary, V. Krishnan, and S. Zafar, “Development of sustainable microwave-based approach to recover glass fibers for wind turbine blades composite waste,” *Resour. Conserv. Recycl.*, vol. 179, 2022, doi: 10.1016/j.resconrec.2021.106107.

[108] Suomen Tuulivoimayhdistys ry, “Tuulivoimaloiden purku ja kierrätys,” 2024. https://tuulivoimayhdistys.fi/tietoa-tuulivoimasta-2/tietopankki/tuulivoimaloiden-purku-ja-kierratys.

[109] J. Li, S. Li, and F. Wu, “Research on carbon emission reduction benefit of wind power project based on life cycle assessment theory,” *Renew. Energy*, vol. 155, 2020, doi: 10.1016/j.renene.2020.03.133.

[110] J. K. Kaldellis and D. Apostolou, “Life cycle energy and carbon footprint of offshore wind energy. Comparison with onshore counterpart,” *Renewable Energy*, vol. 108. 2017, doi: 10.1016/j.renene.2017.02.039.

[111] Y. F. Nassar *et al.*, “Carbon footprint and energy life cycle assessment of wind energy industry in Libya,” *Energy Convers. Manag.*, vol. 300, 2024, doi: 10.1016/j.enconman.2023.117846.

[112] Kitemill, “Taking windpower to new heights,” 2024. https://www.kitemill.com/.

[113] Kitekraft, “Building flying wind turbines,” 2024. https://www.kitekraft.de/airborne-wind-energy.

[114] SkySails, “Wind power: Unleashing its full potential,” 2024. https://skysails-power.com/.

[115] A. Cherubini, A. Papini, R. Vertechy, and M. Fontana, “Airborne wind energy systems: A review of the technologies,” *Renewable and Sustainable Energy Reviews*, vol. 51. 2015, doi: 10.1016/j.rser.2015.07.053.

[116] M. M. Zdravkovich, “Different modes of vortex shedding: An overview,” *J. Fluids Struct.*, vol. 10, no. 5, 1996, doi: 10.1006/jfls.1996.0029.

[117] V. Bladeless, “Bladeless wind power,” 2024. https://vortexbladeless.com/.

[118] J. David and Y. Villarreal, “VIV resonant wind generators,” *Www.Vortexbladeless.Com*, vol. 2, no. 1, 2018.

[119] G. M. Crawley, *Energy storage*, vol. 4. World Scientific Publishing Co. Pte. Ltd, 2017.

[120] C. M. Hoff, *Energy storage technologies and applications*, 1st ed. Artech House, 2022.

[121] J. Warner, *The handbook of lithium-ion battery pack design: Chemistry, components, types and terminology*. 2015.

[122] S. Santhanagopalan, K. Smith, J. Neubauer, G.-H. Kim, M. Keyser, and A. Pesaran, *Design and analysis of large lithium-ion battery systems*, vol. 7, no. 1. 2015.

[123] P. A. Connor, "Batteries for energy storage," in *Energy Storage*, 2017, pp. 117–165.

[124] D. Deng, "Li-ion batteries: Basics, progress, and challenges," *Energy Science and Engineering*, vol. 3, no. 5. 2015, doi: 10.1002/ese3.95.

[125] M. Xie, F. Wu, and Y. Huang, *Sodium-ion batteries: Advanced technology and applications*. 2022.

[126] M. D. Slater, D. Kim, E. Lee, and C. S. Johnson, "Sodium-ion batteries," *Adv. Funct. Mater.*, vol. 23, no. 8, pp. 947–958, 2013, doi: 10.1002/adfm.201200691.

[127] J. Lu, J. Zhang, Y. Huang, Y. Zhang, Y. Yin, and S. Bao, "Advances on layered transition-metal oxides for sodium-ion batteries: A mini review," *Frontiers in Energy Research*, vol. 11. 2023, doi: 10.3389/fenrg.2023.1246327.

[128] M. He *et al.*, "Assessment of the first commercial Prussian blue based sodium-ion battery," *J. Power Sources*, vol. 548, 2022, doi: 10.1016/j.jpowsour.2022.232036.

[129] M. Skyllas-Kazacos, M. H. Chakrabarti, S. A. Hajimolana, F. S. Mjalli, and M. Saleem, "Progress in flow battery research and development," *J. Electrochem. Soc.*, vol. 158, no. 8, 2011, doi: 10.1149/1.3599565.

[130] A. G. Olabi *et al.*, "Redox flow batteries: Recent development in main components, emerging technologies, diagnostic techniques, large-scale applications, and challenges and barriers," *Batteries*, vol. 9, no. 8. 2023, doi: 10.3390/batteries9080409.

[131] W. Wang, Q. Luo, B. Li, X. Wei, L. Li, and Z. Yang, "Recent progress in redox flow battery research and development," *Adv. Funct. Mater.*, vol. 23, no. 8, 2013, doi: 10.1002/adfm.201200694.

[132] C. R. Dennison, H. Vrubel, V. Amstutz, P. Peljo, K. E. Toghill, and H. H. Girault, "Redox flow batteries, hydrogen and distributed storage," *Chimia (Aarau).*, vol. 69, no. 12, 2015, doi: 10.2533/chimia.2015.753.

[133] M. Van de Voorde, *Hydrogen storage for sustainability*, vol. 2. Walter de Gruyter GmbH, 2021.

[134] T. Amirthan and M. S. A. Perera, "The role of storage systems in hydrogen economy: A review," *Journal of Natural Gas Science and Engineering*, vol. 108. 2022, doi:

10.1016/j.jngse.2022.104843.

[135] J. O. Abe, A. P. I. Popoola, E. Ajenifuja, and O. M. Popoola, “Hydrogen energy, economy and storage: Review and recommendation,” *International Journal of Hydrogen Energy*, vol. 44, no. 29. 2019, doi: 10.1016/j.ijhydene.2019.04.068.

[136] Z. Yanxing, G. Maoqiong, Z. Yuan, D. Xueqiang, and S. Jun, “Thermodynamics analysis of hydrogen storage based on compressed gaseous hydrogen, liquid hydrogen and cryo-compressed hydrogen,” *Int. J. Hydrogen Energy*, vol. 44, no. 31, 2019, doi: 10.1016/j.ijhydene.2019.04.207.

[137] I. A. Hassan, H. S. Ramadan, M. A. Saleh, and D. Hissel, “Hydrogen storage technologies for stationary and mobile applications: Review, analysis and perspectives,” *Renewable and Sustainable Energy Reviews*, vol. 149. 2021, doi: 10.1016/j.rser.2021.111311.

[138] D. G. Caglayan *et al.*, “Technical potential of salt caverns for hydrogen storage in Europe,” *Int. J. Hydrogen Energy*, vol. 45, no. 11, 2020, doi: 10.1016/j.ijhydene.2019.12.161.

[139] A. S. Fleischer, “Thermal energy storage using phase change materials: Fundamentals and applications,” *SpringerBriefs Appl. Sci. Technol.*, vol. 0, no. 9783319209210, 2015, doi: 10.1007/978-3-319-20922-7.

[140] M. Mhadhbi, “Introductory chapter: Phase change material,” in *Phase Change Materials and Their Applications*, 2018.

[141] M. K. Rathod and J. Banerjee, “Thermal stability of phase change materials used in latent heat energy storage systems: A review,” *Renew. Sustain. Energy Rev.*, vol. 18, 2013, doi: 10.1016/j.rser.2012.10.022.

[142] M. K. Rathod, “Phase change materials and their applications,” in *Phase Change Materials and Their Applications*, 2018.

[143] S. N. Al-Saadi and Z. Zhai, “Modeling phase change materials embedded in building enclosure: A review,” *Renewable and Sustainable Energy Reviews*, vol. 21. 2013, doi: 10.1016/j.rser.2013.01.024.

[144] S. W. Sharshir *et al.*, “Thermal energy storage using phase change materials in building applications: A review of the recent development,” *Energy Build.*, vol. 285, 2023, doi: 10.1016/j.enbuild.2023.112908.

[145] D. Aydin, S. P. Casey, and S. Riffat, “The latest advancements on thermochemical heat storage systems,” *Renew. Sustain. Energy Rev.*, vol. 41, 2015, doi: 10.1016/j.rser.2014.08.054.

[146] S. W. Sharshir *et al.*, “Effect of copper oxide/cobalt oxide nanocomposite on phase change material for direct/indirect solar energy applications: Experimental investigation,” *J. Energy Storage*, vol. 38, 2021, doi: 10.1016/j.est.2021.102526.

[147] A. K. Thakur *et al.*, “A state of art review and future viewpoint on advance cooling techniques for Lithium–ion battery system of electric vehicles,” *Journal of Energy Storage*, vol. 32. 2020, doi: 10.1016/j.est.2020.101771.

[148] Meyer Turku, “Internal sources.” Turku, 2024.

[149] Maanmittauslaitos, “Karttapaikka,” 2024. https://asiointi.maanmittauslaitos.fi/karttapaikka/.

[150] Entsoe Platform Transparency, “Day-ahead Prices,” 2024. https://transparency.entsoe.eu/transmission-domain/r2/dayAheadPrices/show?name=&defaultValue=true&viewType=GRAPH&areaType=BZN&atch=false&dateTime.dateTime=19.03.2024+00:00%7CCET%7CDAY&biddingZone.values=CTY%7C10YFI-1--------U!BZN%7C10YFI-1--------U&resolu.

[151] Verohallinto, “Sähkön arvonlisäveroa alennetaan väliaikaisesti,” 2022. https://www.vero.fi/tietoa-verohallinnosta/uutishuone/uutiset/uutiset/2022/sahkon-arvonlisaveroa-alennetaan-valiaikaisesti/.

[152] Energiateollisuus, “Sähkön hinta,” 2024. https://energia.fi/energiatietoa/asiakkaat/sahkoasiakkuus/sahkon-hinta/.

[153] Turku Energia, “Hinnastot ja sopimusehdot,” 2024. https://www.turkuenergia.fi/sahkoverkot/hinnastot.

[154] V. V. Mattila, “Merituuli- ja aurinkovoimalat vauhdinotossa,” *Fingrid-lehti*, Jun. 2023.

[155] Suomen Tuulivoimayhdistys ry and Sweco, “Tuulivoimahankkeet Suomessa,” 2024. https://tuulivoimayhdistys.fi/tuulivoima-suomessa/sunnittelussa-olevat-hankkeet.

[156] Motiva, “Tuulivoima Suomessa,” 2024. https://www.motiva.fi/ratkaisut/uusiutuva_energia/tuulivoima/tuulivoima_suomessa.

[157] Energiavirasto, “Aurinkosähkön pientuotanto kasvoi voimakkaasti vuonna 2022,” 2023. https://energiavirasto.fi/-/aurinkosahkon-pientuotanto-kasvoi-voimakkaasti-vuonna-2022.

[158] Motiva, “Aurinkosähköjärjestelmän teho,” 2024. https://www.motiva.fi/ratkaisut/uusiutuva_energia/aurinkosahko/jarjestelman_valinta/aurinkosahkojarjestelman_teho.

[159] Ilmatieteen laitos, “Havaintojen lataus,” 2024. https://www.ilmatieteenlaitos.fi/havaintojen-lataus.

[160] A. Betz, *Introduction to the theory of flow machines*. 1966.

[161] Suomen Tuulivoimayhdistys ry, “Investoinnit,” 2024. https://tuulivoimayhdistys.fi/tietoa-tuulivoimasta-2/tietoa-tuulivoimasta/taloudellisuus/investoinnit.

[162] K. Tiilikainen and H. Säteri, “Valtioneuvoston asetus tuulivoimaloiden ulkomelutason ohjearvoista,” *1107/2015*, 2015. https://www.finlex.fi/fi/laki/alkup/2015/20151107.

[163] Suomen Tuulivoimayhdistys ry, “Äänivaikutukset,” 2024. https://tuulivoimayhdistys.fi/tietoa-tuulivoimasta-2/tietoa-tuulivoimasta/tuulivoiman-vaikutukset/tuulivoiman-ymparistovaikutukset/aanivaikutukset.

[164] Business Finland, “Towards a low-carbon energy system through energy efficiency,” 2024. https://www.businessfinland.fi/en/for-finnish-customers/services/funding/energy-aid.